DISCLAIMER

This report was prepared as an account of work sponsored by an agency of the United States Government. Neither the United States Government nor any agency thereof, nor any of their employees, makes any warranty, express or implied, or assumes any legal liability or responsibility for the accuracy, completeness, or usefulness of any information, apparatus, product, or process disclosed, or represents that its use would not infringe privately owned rights. Reference herein to any specific commercial product, process, or service by trade name, trademark, manufacturer, or otherwise does not necessarily constitute or imply its endorsement, recommendation, or favoring by the United States Government or any agency thereof. The views and opinions of authors expressed herein do not necessarily state or reflect those of the United States Government or any agency thereof. Reference herein to any social initiative (including but not limited to Diversity, Equity, and Inclusion (DEI); Community Benefits Plans (CBP); Justice 40; etc.) is made by the Author independent of any current requirement by the United States Government and does not constitute or imply endorsement, recommendation, or support by the United States Government or any agency thereof.

Optimizing Hydronic Heating for Comfort and Performance in Multifamily Housing

September 2024

Prepared for:

U.S. Department of Energy Building America Program

Office of Energy Efficiency and Renewable Energy

Prepared by:

Joshua Sklarsky

Kurt Roth, Ph.D.

Matthew Kromer

Neil Donnelly

Sankhanil Goswami

New Ecology, Inc.

294 Washington Street, Suite 830

Boston, MA, 02108

September 2024

Suggested Citation:Sklarsky, Joshua., Kurt Roth, Matthew Kromer, Neil Donnelly, and Sankhanil Goswami. 2024. Optimizing Hydronic Heating for Comfort and Performance in Multifamily Housing. Boston, MA. DOE/GO-xxxxxx-xxxx. URL

This material is based upon work supported by the Department of Energy's Office of Energy Efficiency and Renewable Energy (EERE) under the Building Technologies Office under Award Number EE008696, Funding Opportunity Announcement Number DE-FOA-0001824, Building America Industry Partnerships and Research Priorities for High Performance Housing Innovation – 2018.

The work presented in this EERE Building America report does not represent performance of any product relative to regulated minimum efficiency requirements.

The laboratory and/or field sites used for this work are not certified rating test facilities. The conditions and methods under which products were characterized for this work differ from standard rating conditions, as described.

Because the methods and conditions differ, the reported results are not comparable to rated product performance and should only be used to estimate performance under the measured conditions.

Disclaimer

Acknowledgments

The work presented in this report was funded by the U.S. Department of Energy (DOE) Office of Energy Efficiency and Renewable Energy Building Technologies Office.

The research was conducted by the New Ecology, Inc. Building America Team with guidance and support from Fraunhofer Center for Manufacturing Innovation CMI.

The authors thank the following people for their contributions to this effort:

New Ecology, Inc.

Principal Investigator:	Joshua Sklarsky *Former Chief Technology Officer*
Energy Engineers:	Neil Donnelly *Senior Energy Engineer*
	Charles Simek *Energy Engineer*
	Henry Harvey *Former Director of Engineering*
DAQ Engineers:	Sankhanil Goswami *Energy IOT Developer*
	Gregory Hardy-Moss *Technology Associate*
	Theo Brossman *Project Manager*
	Jean Alofan *Field Tech*
Business and Finance:	Marty Josten *Principal Director, Building Decarbonization*
	Edward Connelly *President*
	Alina Michelewicz *Principal Director, Finance and Analytics*

Fraunhofer Center for Manufacturing Innovation CMI

Algorithm Development:	Kurt Roth, Ph.D. *Head, Energy Systems*
	Matthew Kromer *Lead, Grid Integration*
FDD Tool Development:	Matthew Kromer *Lead, Grid Integration*

Department of Energy

DOE Project Officer:	Charles Llenza
DOE Technology Managers:	Jay Wrobel
	Eric Werling
Project Monitor:	Aaron Pott

List of Acronyms

Ambient	Boiler room air temperature
BAS	Building Automation System
CW	Potable cold water supplied to the building
DHW	Domestic Hot Water
DHWR	Potable DHW return temperature
DHWS	Potable DHW supply temperature
DOE	U.S. Department of Energy
DAQ	Data Acquisition
ECM	Energy Conservation Measure
EE	Energy Efficiency
FDD	Fault Detection and Diagnostic
HTG IN	Heating Boiler Loop inlet temperature
HTG OUT	Heating Boiler Loop outlet temperature
HTWR	Space Heating Return Water Temperature
HTWS	Space Heating Supply Water Temperature
HW	Potable hot water temperature leaving tank or water heater delivered mixing valve
HWR (PHWR)	Return water temperature from indirect HX of DHW tank
HWS (PHWS)	Supply water temperature to indirect heat exchanger (HX) of DHW storage tank
MAE	Mean Average Error
NEI	New Ecology, Inc.
OAR	Outdoor Air Reset
OA(T)	Outdoor Air Temperature
ReMO	Remote Monitoring and Optimization
S-W	Summer-Winter
SQL	Sequenced Query Language
TV	Thermostatic Valve
WWSD	Warm-weather-shut-down

Executive Summary

Every central heating and hot water system is unique, often lacking a Building Automation System (BAS) for optimal operation, which leads to inefficient control settings based on estimates. Building operators have long recognized that reducing the heating water supply temperature (HTWS) in response to lower outdoor temperatures can decrease boiler energy consumption. For condensing boilers, this adjustment enhances efficiency by increasing the proportion of heating load met by return temperatures in the condensing regime. However, studies indicate that improved outdoor air reset (OAR) optimization yields only modest savings, less than 2%, with variations in effectiveness across different buildings. Reducing the heating water supply temperature (HTWS) can significantly decrease energy consumption in both condensing and non-condensing boilers by lowering indoor temperatures. Studies have shown that in multifamily buildings, this approach can achieve energy savings of 4% to 16%, though modeling efforts often underestimate actual savings due to overlooked overheating issues.

The potential energy savings from reducing overheating and high space heating loads can significantly surpass those gained from improved boiler efficiency. Monitoring of over 100 multifamily boiler systems revealed that 80% could lower HTWS without compromising comfort. Despite the substantial savings potential, actual savings vary widely, likely influenced by the degree of uncontrolled heat flow in each system. This variability raises the challenge of accurately quantifying expected energy savings from OAR curve changes, which has motivated the development of a software tool to calculate these savings and identify other faults and energy conservation measures (ECMs) effectively.

The project aimed to develop algorithms in a software tool for automating fault detection and optimization analyses in multi-family boiler systems, significantly reducing engineering time and improving cost-effectiveness. The key objectives were:

- to identify faults that could achieve over 15% energy savings
- reduce analysis time by over 80%
- provide accurate weather-adjusted savings estimates
- ensure a payback period of less than three years for optimization efforts.

This would facilitate ongoing commissioning systems in multifamily buildings by lowering implementation costs and demonstrating sufficient savings to qualify as new Energy Conservation Measures in utility programs.

The first project phase developed the Alpha version of the FDD tool, using NEI's manual processes to analyze hydronic boiler data. This basic version was intended for initial testing and iteration, built in Python for future integration into commercial platforms. Following Alpha feedback, we created a more advanced Beta version, using both NEI’s existing field data and

newly installed systems, suitable for wider testing and commercialization, focusing on tool validation and deployment planning. The Beta version is ready for broader application, with updated documentation and recommendations for future improvements based on field data and user feedback.

Meeting the project objectives will enable widespread deployment of ongoing commissioning systems for multifamily boilers by reducing implementation costs and demonstrating favorable savings-to-investment ratios for qualifying as new Energy Conservation Measures (ECMs). We developed algorithms that analyze boiler data, identify energy-wasting faults, and predict annual energy savings from operational changes.

The Fault Detection and Diagnostic (FDD) tool, created in Python, ingests data from PostgreSQL databases, applies FDD algorithms, and generates recommendations. Through testing with NEI's field data, we refined the algorithms and improved data visualizations for quick issue triage. Initially focused on space heating, the tool expanded in Phase 2 to include Domestic Hot Water modules for combined systems. We also enhanced energy savings predictions by integrating building physics, addressing measurement inaccuracies, and enabling evaluation of multiple ECMs using TMY data for forecasting.

Through testing on existing data sets, we have shown that the FDD tool can identify the following key faults, each implemented as a software module:

Suboptimal Outdoor Temperature Sensor Placement ("Suboptimal Tout") – Detects missing or poorly placed outdoor temperature sensors.

Outdoor Air Reset (OAR) Issues – Identifies missing or misconfigured OAR curves.

Warm Weather Shutdown and Summer-Winter Switch ("WWSD/SW-Switch") – Detects inactive or misconfigured warm weather shutdown and seasonal switching.

Excess Boiler Cycling ("Excess Cycling") – Identifies instances of excessive boiler cycling.

Domestic Hot Water (DHW) Setpoint Misconfiguration – Detects improper DHW setpoints.

One of the most important aspects of this tool is the ability to measure and quantify the energy saved from the implementation of the ECM. The key features related to this are as follows:

Prior Savings: NEI's work on 100+ buildings in Massachusetts showed 80% realized an average of 11% energy savings from remote monitoring and optimization.

Modeled Estimates: The tool uses engineering models to compare baseline and ECM cases, estimating energy savings through changes like OAR curve and boiler settings.

Updated OAR Model: Early models assumed perfect control of heat flow. The updated version accounts for building overheating, refining energy savings estimates.

Updated ECM Data Model: Ingests an configuration file that specifies combinations of ECMs (OAR settings, WWSD settings, and temperature sensor placement) to evaluate the impact of remediation.

Tool Performance: Comparing the tool's analysis to manual methods, it matched 85% of assessments, with high accuracy for OAR curve and temperature sensor faults, though false positives were common.

NEI's manual analysis of over 100 monitored sites for the Massachusetts Clean Energy Center(MassCEC) project took about 10 hours per site, down from the original 16-20 hours, with three hours spent on data QC and fault evaluation. The FDD tool significantly reduces this time, allowing a full site analysis in just three minutes. It automates QC, fault detection, and heating curve evaluation, enabling more frequent analysis and quicker response to operational issues. A batch of five sites can be analyzed in 10 minutes, with an additional 40 minutes to review outputs, representing a 94% reduction in time compared to manual methods.

To validate the model, NEI applied it to 19 OAR curve and WWSD changes at 12 Massachusetts sites using ReMO platform data. Sites were limited to those with boilers serving only space heating. Pre-ECM and post-ECM periods were compared to predict energy consumption after OAR curve adjustments. Modeled savings were 12.8%, and observed savings were 11.3%, with an average difference of 4.3%. The model predicted savings within ±5% for 13 changes and within ±10% for 16 changes, showing it effectively captures the energy impact of boiler overheating and OAR curve changes.

The Simple Payback Period (SPP) is calculated by dividing boiler optimization costs by the resulting cost savings. For nine multi-family properties, with an average annual space heating cost of $11,000 and DHW heating cost of $7,000, a 15% savings yields an SPP of 2.6 years. However, changes since the study such as rising hardware, labor, and natural gas costs, along with supply chain challenges make current SPP difficult to estimate. Decarbonization and electrification efforts also affect the relevance of gas-fired boilers, potentially shortening the payback window before electrification occurs. Additionally, reactive maintenance and tenant complaints may lead to overrides, reducing ECM persistence.

With the rapid shift towards electrification and the increased adoption of heat pumps, the FDD tool is well-positioned to optimize existing systems, delivering quick savings in the short term while also facilitating the implementation of electrification initiatives through its detailed understanding of actual building heating loads. This support is critical for selecting new equipment that is appropriately sized for specific loads, offering substantial initial cost-saving opportunities and ensuring more efficient operation through improved load matching, an issue frequently observed in current building data. Since high-efficiency condensing boilers remain the most cost-effective option for many multi-family buildings, and fossil fuel-based systems are still widespread, the FDD tool will continue to be a valuable resource for fault detection and system optimization, maximizing energy savings.

With these dual pathways for building heating and hot water systems, the FDD tool is capable of serving buildings with their current systems for as long as they remain in use, while also supporting a seamless and efficient transition to newer technologies. The methods developed within the FDD tool can be adapted to future electrified systems, evolving as needed to drive further optimization and address the common challenge of system overrides, which affect all types of systems.

Table of Contents

List of Figures

List of Tables

Introduction

Every central heating and hot water system is unique. They are custom designed, plumbed, and installed by teams with a range of technical capability. When there is no Building Automation System (BAS) dynamically controlling system operation, individual pieces of equipment (e.g., boilers, pumps, etc.) are left to operate with little or no data feedback. Control settings are based upon settings used at other buildings and best estimates and are not typically optimized based on actual operating data.

Yet, building operators have realized for several decades that boiler energy consumption for space heating can be reduced by reducing (aka resetting) the heating water supply temperature (HTWS) as the outdoor air temperature (Tout) decreases (see Figure 1, from Landry et al. 2021).

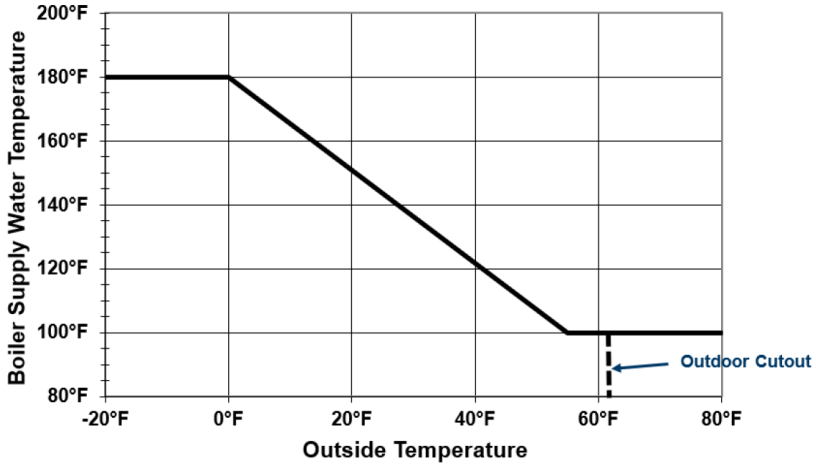

Figure 1: Example of an outdoor air reset (OAR) curve; from Landry et al. 2021

For condensing boilers, this can increase the portion of the space heating load met by heating water return temperatures (HTWR) that occur in the condensing regime, increasing boiler efficiency, η (see Figure 2, where HTWR = "Inlet water temperature"; from ASHRAE 2020).

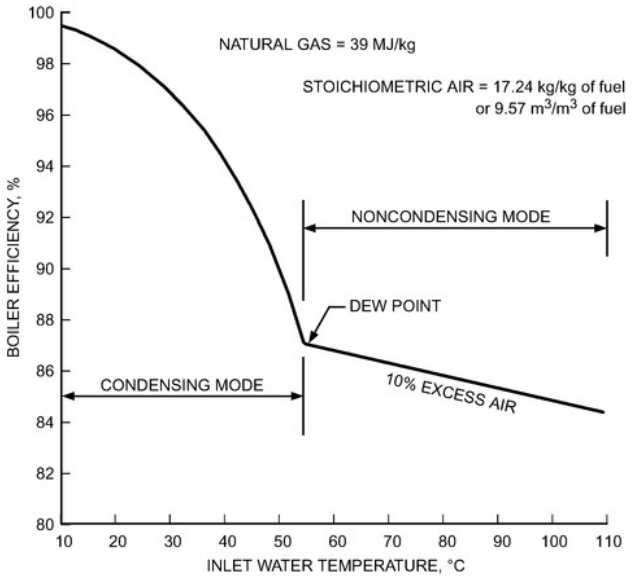

Figure 2: Example of how condensing boiler efficiency varies as a function of inlet water temperature; (from ASHRAE 2020)

Although condensing boilers can realize large efficiency-related savings when replacing non-condensing boilers, the efficiency-driven savings from improved outdoor air reset (OAR) optimization is quite modes. For example, modeling of the expected efficiency-driven savings for 17 monitored commercial condensing boiler systems found that improved reset curve parameters would reduce space heating energy consumption by less than 2% at all sites (Landry et al. 2021), while another study by the same organization found an average of ~1.5% efficiency-related savings at 10 sites from reset curve changes (range: 0-4%; Landry et al. 2016).[1]

In both condensing and non-condensing boilers, reducing HTWS at a given T_{out} can also reduce space heating energy consumption by reducing indoor temperature (T_{in}) and, consequently, effective space heating loads, Q_{in}. As a field study by Hewett and Peterson (1984) found, boiler systems are prone to overheating spaces due to a combination of high T_{in} preferences by inhabitants (sometimes accompanied by window opening), failed thermostatic zone valves (TV), and/or poorly or uninsulated distribution piping that result in uncontrolled heat flow to spaces. They showed that reducing HTWS(T_{out}) in multifamily buildings served by cast-iron boilers decreased space heating energy consumption by between 4 and 16%, with a corresponding 1 to 4ºF decrease in T_{in} measured in hallways. Figure 3 below shows how daily boiler energy consumption as a function of daily T_{out} changed in the building that achieved the greatest savings (when combined with a warm-weather shut-down [WWSD] temperature of T_{out} = 55ºF; Hewett and Peterson 1984).

1 We found similar results when analyzing OAR curve changes for >10 buildings, using manufacturer data for boiler efficiency, η(HTWS), hourly TMY Tout data, and assuming space heating loads decreased linearly from the design temperature, Tout,design, to a balance temperature, Tbal = 60oF.

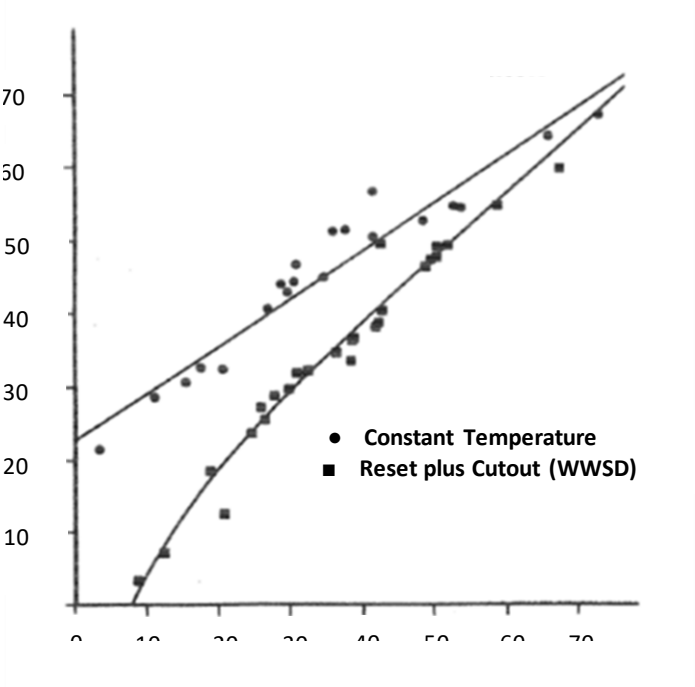

Figure 3: Field data for boiler daily energy consumption as a function of heating degree days for boilers with constant (top curve) and reset (lower curve) control; recreated from Hewlett and Peterson (1984).

Existing industry rules of thumb range from 1% savings per 1°F reduction in HTWS to "reduce 4°, save 1%"[2]. Beyond such basic approaches, Landry et al. (2021) attempted to model the energy savings from decreasing OAR curve parameters based on the energy savings found in prior studies for OAR curve changes, including Hewett and Peterson (1984). They found a limited correlation between modeled and actual savings, on average underestimating savings by 40% (see Figure 3). This likely occurs because that model does not model the *actual* building overheating ("load reduction savings") occurring in specific buildings.

[2] See: https://www.heat-timer.com/outdoor-reset-control-savings/ for the latter; the 1°F = ~1% savings comes from discussions with practitioners.

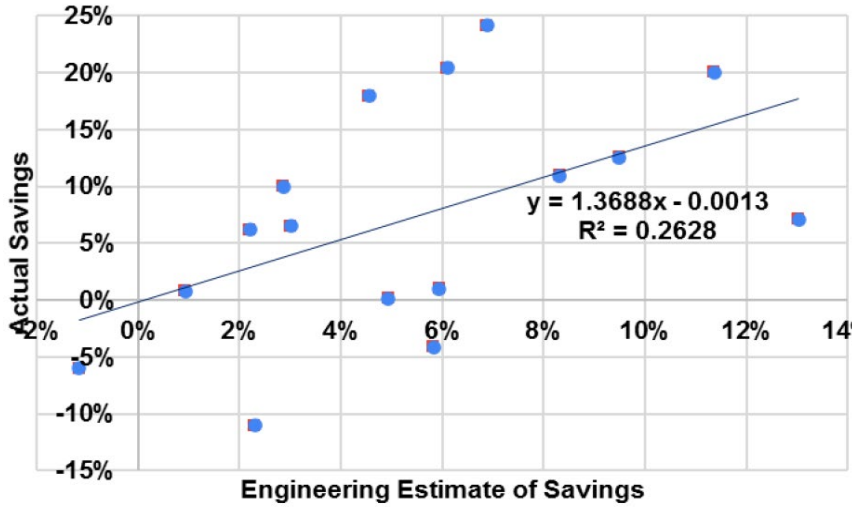

Figure 4: Engineering estimates versus actual savings for commercial boiler systems, from Landry et al. (2021). The engineering estimates underestimated actual energy savings by an average of 40%

Clearly, the energy savings potential from reducing overheating and the resulting high space heating loads can greatly exceed those from increasing boiler efficiency. Furthermore, the prevalence appears to be acute in the roughly 2 million multi-family building with hydronic heat[3], i.e., monitoring of >100 multi-family boiler systems in colder climates by New Ecology (2018) found that in 80% of them HTWS could be lowered without compromising comfort. Although the savings potential can be large from OAR curve changes, the realized savings varies greatly among buildings (Hewett and Peterson 1984, Davey and Connelly 2018, New Ecology 2018). Presumably, this varies with the degree of uncontrolled heat flow of that specific boiler system. The challenge then becomes: how does one accurately quantify the expected energy savings from potential changes to the OAR curve?

This is one of the central questions that led this project team down the path to develop a software tool that can not only calculate these savings, but identify other faults and ECMs, in a cost-effective manner.

Data Acquisition System

We include a summary of the sensors now typically deployed to help readers follow technical discussions that follow.

[3] The 2020 DOE EIA RECS estimated that 2.8 million buildings with 5+ units have steam or hot-water heating systems, primarily in colder climates; we expect that a sizeable majority are hot-water systems.

Table 1: Standard sensor package deployed in installations

Sensor	Description
HTWS	Space heating supply water temperature
HTWR	Space heating return water temperature
HTG IN	Heating Boiler Loop inlet temperature
HTG OUT	Heating Boiler Loop outlet temperature
DHWS	Potable DHW supply temperature
DHWR	Potable DHW return temperature
HW	Potable hot water temperature leaving tank or water heater delivered mixing valve
CW	Potable cold water supplied to the building
HWS[4] (PHWS)	Supply water temperature to indirect heat exchanger (HX) of DHW storage tank
HWR (PHWR)	Return water temperature from indirect HX of DHW tank
Ambient	Boiler room air temperature
OA	Outdoor air temperature (only installed in non-Modbus installations)

Figure 5 shows example sensor installations for both combined and separate systems (connections to the Ambient and OA sensors not shown).

[4] HWS and HWR are the sensor names used in combined heating and DHW systems, while PHWS and PHWR are used in separate systems (P for potable).

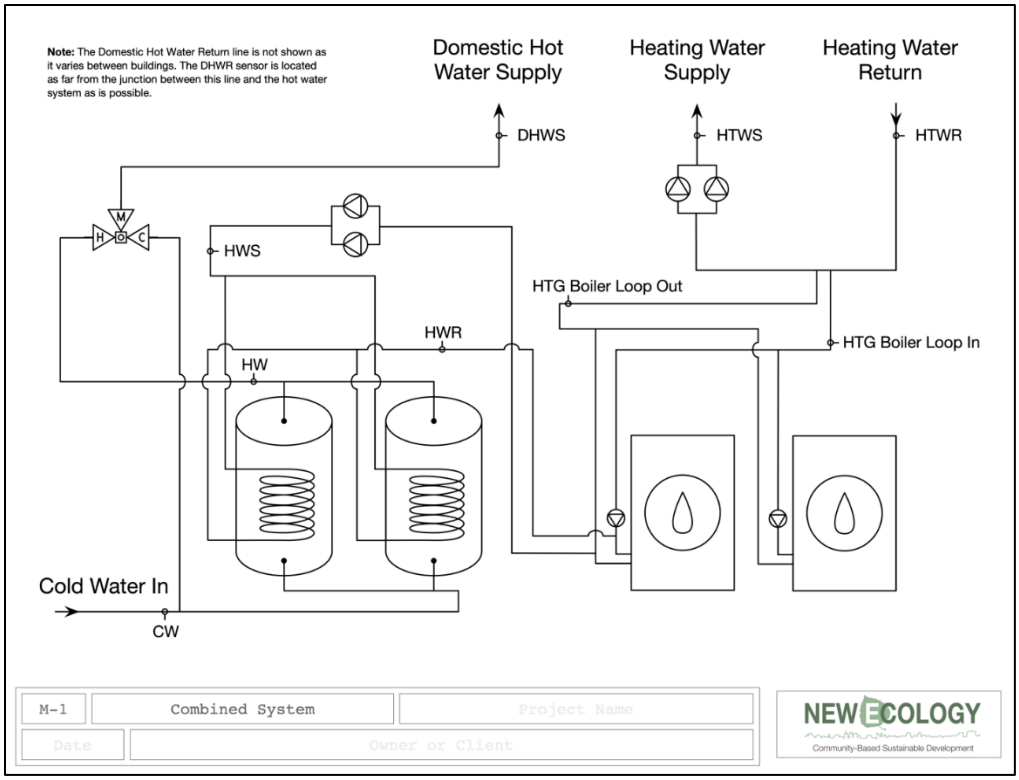

Figure 5: Sensor location diagram for a combined boiler system

When the equipment on site has the capability for communications through industrial BAS protocols such as MODBUS[5], we can connect and integrate those data into our database. In addition, the original deployment also allowed us to install relays on each non-MODBUS capable boiler to provide boiler on/off data; those relays are not part of the current DAQ specification.

[5] The Modbus protocol is a standard employed by many boiler manufacturers to communicate with controllers. Through this interface, a DAQ system is able to monitor and record the same internal sensor data a boiler may expose to its controller. See www.modbus.org for further details.

Methodology

This project sought to develop and implement algorithms in a software tool that automates the fault detection and optimization analyses and processes for multi-family boiler-system optimization to significantly reduce the engineering time required to perform such analyses. This will improve the cost-effectiveness and scalability of multi-family boiler-system optimization and, hence, the energy savings realized.

The primary goal of this project was to remove cost barriers that currently prevent building operators in multi-family buildings from gaining operational insight that can lead to energy and maintenance savings. To achieve this goal, we identified the following four objectives:

1. Identify faults and recommendations that can achieve an average of 15%+ reduction in space heating energy consumption
2. Reduce analysis time by 80%+ relative to manual approaches
3. Calculate weather-adjusted energy savings estimates that will be within ±20% of achieved energy savings, based on pre-ECM and post-ECM gas consumption data.
4. Achieve less than a three-year payback period for boiler optimization.

These objectives would enable the widespread deployment of ongoing commissioning systems for multifamily boiler systems by 1.) reducing the cost of implementing systems in the field and 2.) demonstrating sufficient savings-to-investment ratios for the system to qualify as a new Energy Conservation Measure (ECM) in utility energy efficiency (EE) programs.

The first phase of the project focused on developing the Alpha version of the FDD tool, leveraging extensive existing investments by NEI in developing manual processes to analyze the minute-level hydronic boiler system data. The Alpha version was intended to be a basic, functional version of the tool that could be used for initial testing, refinement, and iteration. We planned to develop software using an open-source programming language (Python), so the resulting modules could later be integrated into commercial software tools or enterprise platforms. Since the innovation in this project is primarily related to the automated discovery and quantification of ECMs, this effort relied on manual data input and static output report files. Interactive graphical user interface development was premature at that stage (while variables, inputs, and outputs were fluid), but was to be considered in a later phase.

Based on feedback from Alpha testing, we developed a more mature Beta version of the tool that was suitable for wider field testing and ready for integration into a commercially viable platform. Phase 2 of the project focused on developing the Beta version of the tool, tool validation, and a Commercialization Plan to scale tool deployment. Development of the Beta version leveraged feedback and results from Alpha field-testing efforts to improve and refine the tool. The outcome of the Beta version development was a software tool ready for more widespread testing, pilot applications, and eventually, integration into a commercially viable platform. Software documentation was updated for the Beta version. Based on field testing of the Beta version using

both NEI's existing field data and newly installed systems, as well as end-user feedback, we developed a list of recommendations for future software updates and development for commercialization.

Results

Meeting the objectives listed above would enable the widespread deployment of ongoing commissioning systems for multifamily boiler systems by 1) reducing the cost of implementing systems in the field and 2) demonstrating sufficient savings-to-investment ratios for the system to qualify as a new Energy Conservation Measure (ECM) in utility energy efficiency (EE) programs.

We have synthesized the expert knowledge from NEI's analysts and the technical literature with physics-based models to develop algorithms that analyze boiler system data and identify several high-priority, energy-wasting faults listed below. In addition, we developed algorithms that predict how changes to boiler system operating parameters affect boiler energy consumption, allowing us to predict the annual energy savings from specific parameter changes.

We then created a Fault Detection and Diagnostic analysis tool ("FDD Tool") in python that can ingest incoming data streams from a continuously updating PostgreSQL time-series database or archived database of site-installed sensors, apply the FDD algorithms, and generate recommendations.

Figure 6 and Figure 7 depict the overall flow of the tool and the types and the data taxonomy for information flowing into the tool. Depending on the data available from a specific system, the tool can work with different data inputs; we presented recommendations for sensor packages based on available sensor data and a discussion of the trade-offs for the different fault detection algorithms based on available data in the "Updated DAQ Specification and Data Requirements" submitted to DOE (See Appendix A).

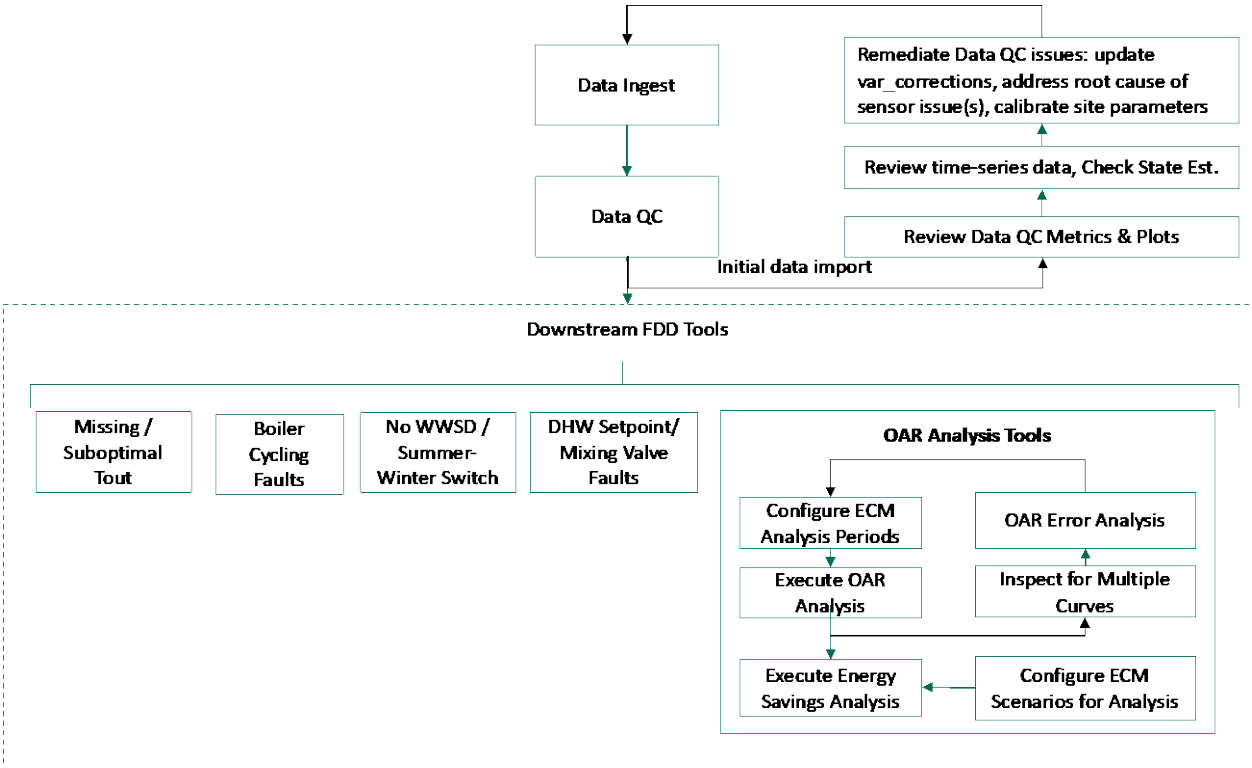

Figure 6: Boiler analysis tool flowchart

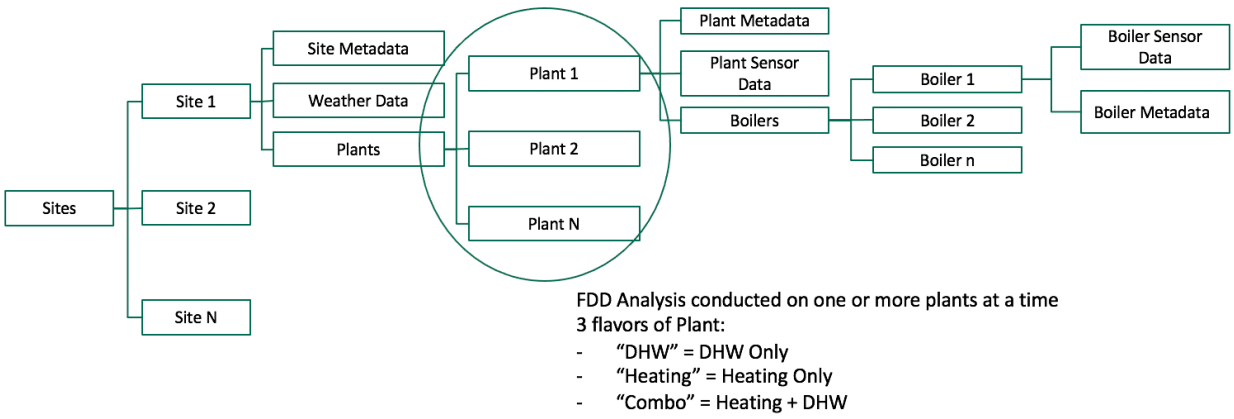

Figure 7: Boiler analysis tool data taxonomy

Through testing the tool on existing NEI field data sets, we have refined the algorithms, particularly the thresholds used to identify faults and to infer the operational status of boiler system components (e.g., boiler pumps), and to incorporate feedback from NEI analysts to create? effective and intuitive data visualizations that enable rapid triage of potential issues. Phase 1, the tool focused primarily on space-heating faults, foremost in boilers serving space heating alone. In Phase 2, further work on the Domestic Hot Water modules was completed, notably for combination systems, i.e., those where boilers serve both space and water heating loads. The FDD tool also provides a full suite of analysis and recommendations to optimize heating plants that serve both heating and DHW needs ("combined" plants), and a narrower

range of analysis and recommendations to optimize DHW operation (whether as part of a combined heating + DHW or standalone DHW plants).

Our testing found that combined plants present a more challenging use case than standalone heating plants.

Finally, a major component of the work done in Phase 2 involved developing new approaches to greatly improve the energy savings prediction toolset to: (1) incorporate a more accurate model of the underlying building physics; (2) account for the downstream impact of inaccurate boiler outdoor air temperature (T_{out}) measurements on estimates; (3) integrate savings estimates from implementation of multiple ECMs into a composite summary; (4) implement a new data model that enables a user to evaluate the impact of a portfolio of ECMs; and (5) incorporate use of TMY data for forward-looking predictions.

Discussion

A discussion of the progress we made towards meeting each objective below follows.

Objective 1: Identify faults and recommendations that can achieve an average of 15%+ reduction in space heating energy consumption

Through testing on existing data sets, we have demonstrated that we can identify the following key faults, each implemented as a software module in the FDD tool:

1. Missing or suboptimal outdoor temperature sensor placement ("Suboptimal T_{out}")
2. Missing or misconfigured outdoor air reset (OAR) curves ("OAR")
3. Inactive or misconfigured warm weather shutdown (WWSD) and/or Summer-Winter Switch ("WWSD/SW-Switch")
4. Excess Boiler Cycling ("Excess Cycling")
5. Misconfigured DHW setpoints ("DHW Setpoint")

Examples and discussion of each fault detection module follow.

1. Missing or suboptimal outdoor temperature sensor placement ("Suboptimal T_{out} ")

This fault mode occurs when a site's outdoor temperature sensor is either unavailable or presents data quality issues. The FDD tool addresses two classes of data quality issues: sensors errors (e.g., sensor readings do not change and/or report out of range values); and issues with sensor placement. Sensor placement errors are detected by comparing local (onsite) temperature measurements with publicly available weather station data, e.g., from the National Weather Service.

The script generates a table () showing the following metrics. The output of the table varies depending on whether analysis is conducted over the whole data capture (show_by_analysis_pd = False,) or conducted by ECM Analysis Period (show_by_analysis_pd=True, see).

- **Index column:**

  For analysis conducted over the full data captured, the index is:

  <site>-<plant_id>-'All' (for all data)

  <site>-<plant_id>-'Last 12 Months' (for last 12 months)

  if analysis conducted by ECM Analysis Period, the index is:

  <site>-<plant_id>-<ECM Analysis Pd Idx>

- **ECM Idx, ST, ET:** Zero-indexed reference to the ECM Analysis period, with a value of zero referencing the most recent data.

- **LastGoodReading:** Last Valid Data Point.
- **SensorError%**: Sensor error is defined as either an out of range (non-physical) measurement or "invariant" sensor data (defined as < 3 deg delta between weekly max/min reading). The output is coded red if more than 10% of hours in the last 12 months have a sensor error (for analysis conducted over full data capture), or if more than 10% of hours have a sensor error (for analysis conducted by ECM Analysis Period).
- **%HrsOutOfRange:** An "hour out of range" is defined as an hour in which there is >10 ^{o}F discrepancy between the onsite Tout sensor and the weather station temperature reading.
- **ValidHrs:** Number of hours for which a valid t_out reading was returned in this analysis period. Coded red if there are fewer than 1000 hrs for analysis.

The t_out evaluation metrics compare the average error and mean average error (MAE) of t_out to t_weather_station measurements using several different data segmentation parameters:

- **Active Pts vs All Pts:** If "-Active" is appended to the column name, the error includes only points where the heating plant is ON. If "-Active" is not appended to the column name, the error includes all data points (heating plant ON and OFF). Intuitively, one might expect that focusing on temperature errors during active plant operation are the most relevant metric, as active operation is what drives energy consumption. However, looking at ONLY active points can mask a class of issues in which warm weather shutdown occurs at the incorrect temperature due to bad local temperature measurements.
- **Time of day:** Used to identify errors that vary based on diurnal factors, such as solar loading. Data is grouped into three segments: 00:00 to 10:00 (nighttime), 10:00 to 15:00 (morning), and 15:00-24:00 (afternoon/evening). *Note: times are in UTC, so subtract four to five hours to convert to eastern time.*[6]
- **AvgErr vs MAE:** Results for both average and mean average error shown. We found that Average Error is generally more predictive of the type of systematic issue that we are trying to identify.
- **AvgErr-Active/MAE-Active:** Average/Mean Average Error across the full data set, including only heating plant "ON" points.
- **AvgErr, MAE:** Average/Mean Average Error across the full data set, including heating plant "ON" and "OFF" points.

6 Note: this logic is currently hard-coded for eastern time zone. It would need to be updated for other time zones.

- **1500-2400-Active / 0000-1000-Active / 1000-1500-Active:** Average Error across specific times of day, including only heating plant "ON" points.
- **1500-2400 / 0000-1000 / 1000-1500:** Average Error across specific times of day, including heating plant "ON" and "OFF" points.
- **bad_** T_{out}**:** Set to True if any of the following conditions are met:
  - Absolute value of AvgErr-Active is greater than 2.5 ^{o}F
  - Absolute value of AvgErr is greater than 2.5 ^{o}F
  - Absolute value of three or more of the time-of-day error metrics[7] is greater than 2.5 ^{o}F

7 i.e., 1500-2400-Active / 0000-1000-Active / 1000-1500-Active / 1500-2400 / 0000-1000 / 1000-1500

ECM Idx	ST	ET	LastGoodReading	ValidHrs	SensorErr%	%HrsOutOfRange	AvgErr-Active	AvgErr	MAE-Active	MAE	1500-2400-Active	0000-1000-Active	1000-1500-Active	1500-2400	0000-1000	1000-1500	bad_tout
All	2017-01-12	2019-06-18	2018-06-22	12,276	33%	7%	0.8	2.8	3.7	5.0	1.7	0.9	-0.6	5.7	2.1	-0.1	True
Last12Months	2018-06-18	2019-06-18	2018-06-22	89	99%	0%	-1.8	0.0	1.9	1.8	nan	-1.8	nan	0.7	-0.8	0.6	False
All	2017-01-03	2019-02-28	2019-02-28	17,773	0%	2%	1.3	0.9	2.7	2.9	2.1	2.0	-1.2	1.8	1.7	-2.2	False
Last12Months	2018-02-28	2019-02-28	2019-02-28	8,238	0%	2%	0.7	0.3	2.4	2.8	1.4	1.4	-1.7	1.2	1.1	-2.8	False
All	2017-01-03	2022-01-28	2022-02-17	41,326	0%	9%	2.4	1.6	4.7	4.7	0.9	5.2	-1.8	-0.0	4.8	-3.0	True
Last12Months	2021-02-18	2022-01-28	2022-02-17	7,755	0%	2%	-0.0	-0.3	3.4	3.5	-0.3	1.9	-4.3	-0.5	1.8	-4.5	False

Figure 8: Suboptimal T_{out} – Sample output for analysis conducted over full data capture

ECM Idx	ST	ET	LastGoodReading	ValidHrs	SensorErr%	%HrsOutOfRange	AvgErr-Active	AvgErr	MAE-Active	MAE	1500-2400-Active	0000-1000-Active	1000-1500-Active	1500-2400	0000-1000	1000-1500	bad_tout
0	2018-09-28	2019-06-18	None	0	100%	0%	nan	nan	nan	nan	nan	nan	nan	nan	nan	nan	False
1	2017-11-05	2018-06-22	2018-06-22	5,236	0%	0%	-0.5	-0.2	1.7	1.8	0.2	-0.5	-1.4	0.6	-0.3	-1.2	False
2	2017-01-12	2017-06-15	2017-06-30	3,992	0%	20%	2.5	4.4	6.9	7.9	4.1	2.5	0.5	8.1	3.6	0.5	True
0	2018-01-08	2019-02-28	2019-02-28	9,369	0%	2%	0.9	0.5	2.5	2.8	1.6	1.6	-1.5	1.3	1.3	-2.5	False
1	2017-03-17	2018-01-07	2018-01-07	6,683	0%	2%	1.6	1.2	2.9	3.1	2.9	2.2	-1.2	2.3	2.0	-2.2	False
2	2017-01-03	2017-03-16	2017-03-16	1,554	0%	2%	2.4	2.3	3.2	3.2	2.9	3.4	-0.3	2.8	3.1	-0.4	True
0	2021-01-07	2022-02-18	2022-02-17	8,756	0%	2%	0.2	-0.3	3.4	3.4	-0.2	2.1	-3.8	-0.5	1.8	-4.3	False
1	2018-09-15	2021-01-06	2021-01-06	19,602	0%	12%	2.9	2.1	5.1	5.1	1.0	6.0	-1.4	0.1	5.6	-2.5	True
2	2017-01-03	2018-09-14	2018-09-14	12,963	0%	11%	3.2	2.0	5.1	5.2	1.6	6.0	-1.0	0.1	5.7	-2.9	True

Figure 9: Suboptimal T_{out} – Sample output for analysis conducted by ECM Analysis Pd

The Suboptimal T_{out} script also generates a series of plots () for each site that includes: (1) time series of T_{out}, weather station, and error; (2) frequency of "Hours out of Range" > 10 °F, by month; and (3) a heatmap of error by hour of the day for different periods of the year (All Year / Oct-May / Jun-Sep):

- If analyzing the full data capture, the heatmap displays data for (a) the full data capture period and (b) the last 12 months of data.
- If analyzing data by ECM Analysis Period, the heatmap displays data for (a) all data within in the ECM Analysis Period, and (b) Heating On-only points within the ECM Analysis period. The (top) error frequency plot shows error frequency for all points (blue) and for heating on-only points (red).

In the example shown below, there appear to have been a substantial placement issue in 2017, as evidenced by the frequency of hours out of range throughout 2017 (see first half of the plots in rows 1 and 2), with the error likely due to excess solar gains (row #3). As shown in row #4, which shows an hourly heatmap for only the most recent 12 months, it appears that the error has since been corrected.

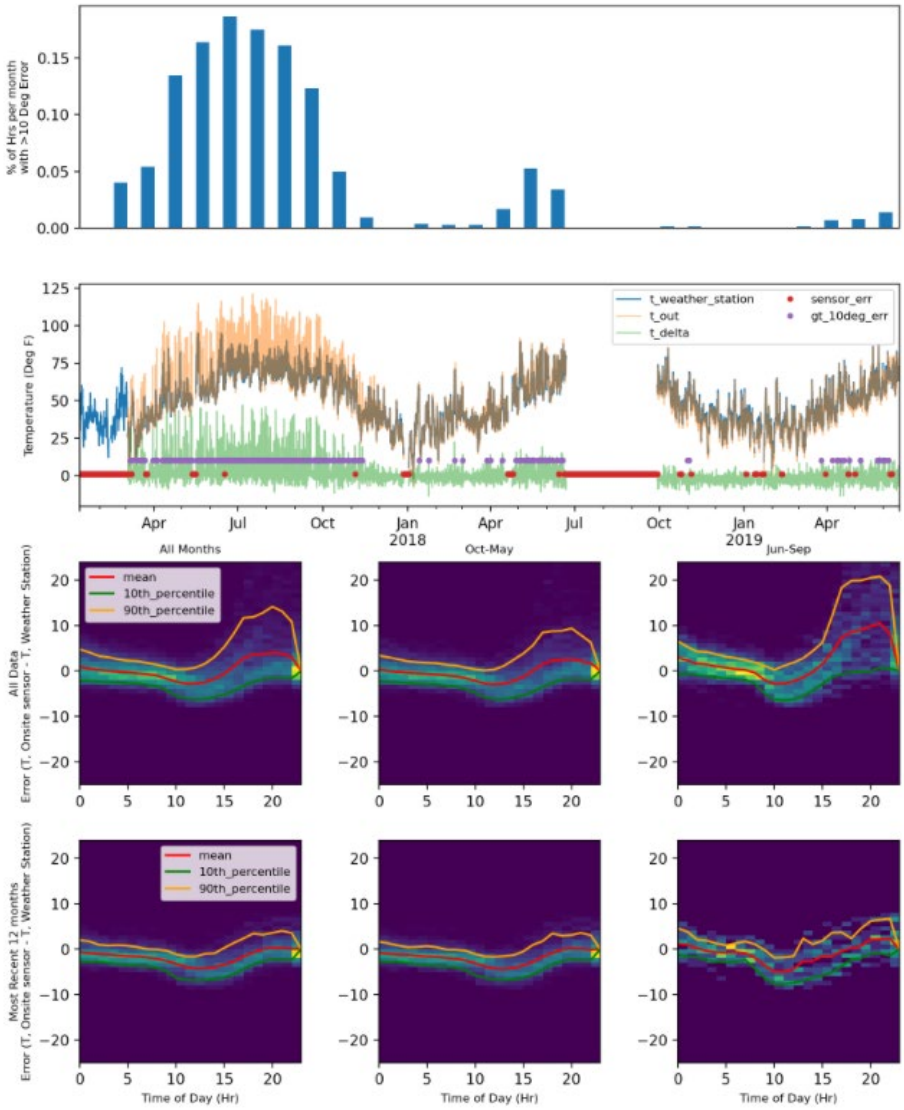

Figure 10: Example Suboptimal T_{out} Plots

2. Missing or misconfigured outdoor air reset (OAR) curves ("OAR")

The OAR Analysis provides feedback about OAR performance for a cohort of sites, both for sites with and without a known/expected OAR curve. For sites without a configured OAR, it extracts an implied OAR curve by fitting OAR parameters to observed data and then provides feedback as to whether the observed curve parameters fit within a valid operating window. For sites that have an OAR curve specified, the tool compares the observed OAR behavior to the expected behavior implied by the specified curve. Since OAR curves can change over time, e.g., from user overrides, the tool evaluates OAR curves at different points in time.

To accomplish this, the tool generates a series of data visualizations and analyses that characterize plant operation across multiple dimensions, including OAT-vs-HTWS trends, WWSD temperature, S-W Switch status, qualitative assessment of t_out placement, and DHW state estimation for combination plant. In combination, these toolsets allow a user to estimate plant configuration settings over time and estimate the energy impact of proposed or previously implemented configuration changes.

An OAR Analysis is performed on one or more "ECM Analysis Periods". An ECM Analysis Period can be configured to automatically segment a data set by heating season, by OAR configuration date(s), or using a custom set of dates.

The OAR Analysis tool generates two different data visualizations of the OAT-vs-HTWS trend: a scatter plot visualization and a heatmap visualization.

The scatter plot data visualization () is implemented as a 2x2 matrix of scatter plots for each combination of HTWS key (t_htws / t_system_supply) and outdoor air temperature (Onsite OAT ("t_out") / Weather Station OAT ("t_weather_station"), with each ECM Analysis Period represent with a different color. If an end point is not available for the plant under evaluation, the plots associated with that plant will be blank. Each ECM Analysis Period in each scatter plot is overlaid with a parameterized OAR curve (either derived or configured) associated with that time period. If a configured OAR curve is available, the configured curve is overlaid on each plot. If the analysis uses a derived curve, the following logic drives the curve overlay:

- If t_htws and t_weather_station are available, HTWS/WS is overlaid on HTWS/WS scatter plot[8]
- If t_system_supply and t_out are available, SST/ T_{out} is overlaid on SST/ T_{out} scatter plot[9]
- The "primary" curve fit (i.e., t_htws_primary / t_out_primary) is overlaid on HTWS/ T_{out}, and SST/WS scatter plots

The scatter plot includes any points where the plant state estimation detects the plant is active: for heating plants, this should correspond only to active heating calls; for DHW plants it includes heating-only and DHW calls (plant_state=125 or plant_state=175). However, the derived curve fit is extracted using only data points that are heating only (plant_state=125).

8 This plot represents a user perspective on heat delivery to the building: it shows actual outdoor temperature conditions plotted vs actual supply temperature delivered to the heating loop

9 This plot represents a control-based perspective on heat delivery: it shows the primary boiler control variable (t_out) plotted vs the primary output that the boiler controls (t_system_supply)

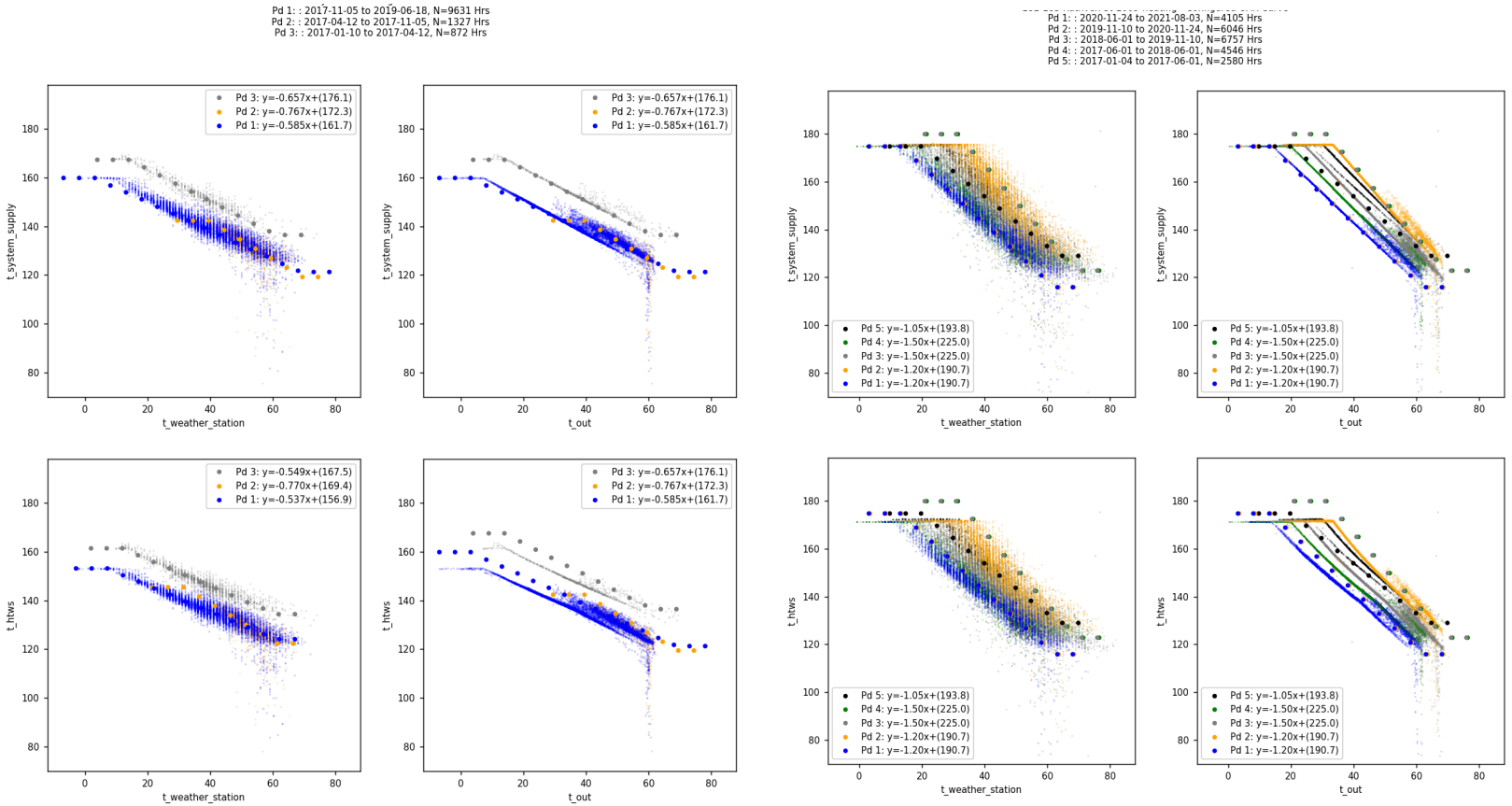

Figure 11: Example scatter plot data visualization for a set of derived curves (left-hand plot) and configured curves (right—hand plot)

The heatmap data visualization () generates a single heatmap of t_out_primary vs t_htws_primary for each ECM Analysis Period.[10] For sites with a configured OAR curve, an additional plot of (median error + 100 deg) as a function of OAT is displayed.

10 Note that the most recent ECM Analysis Period is indexed to zero

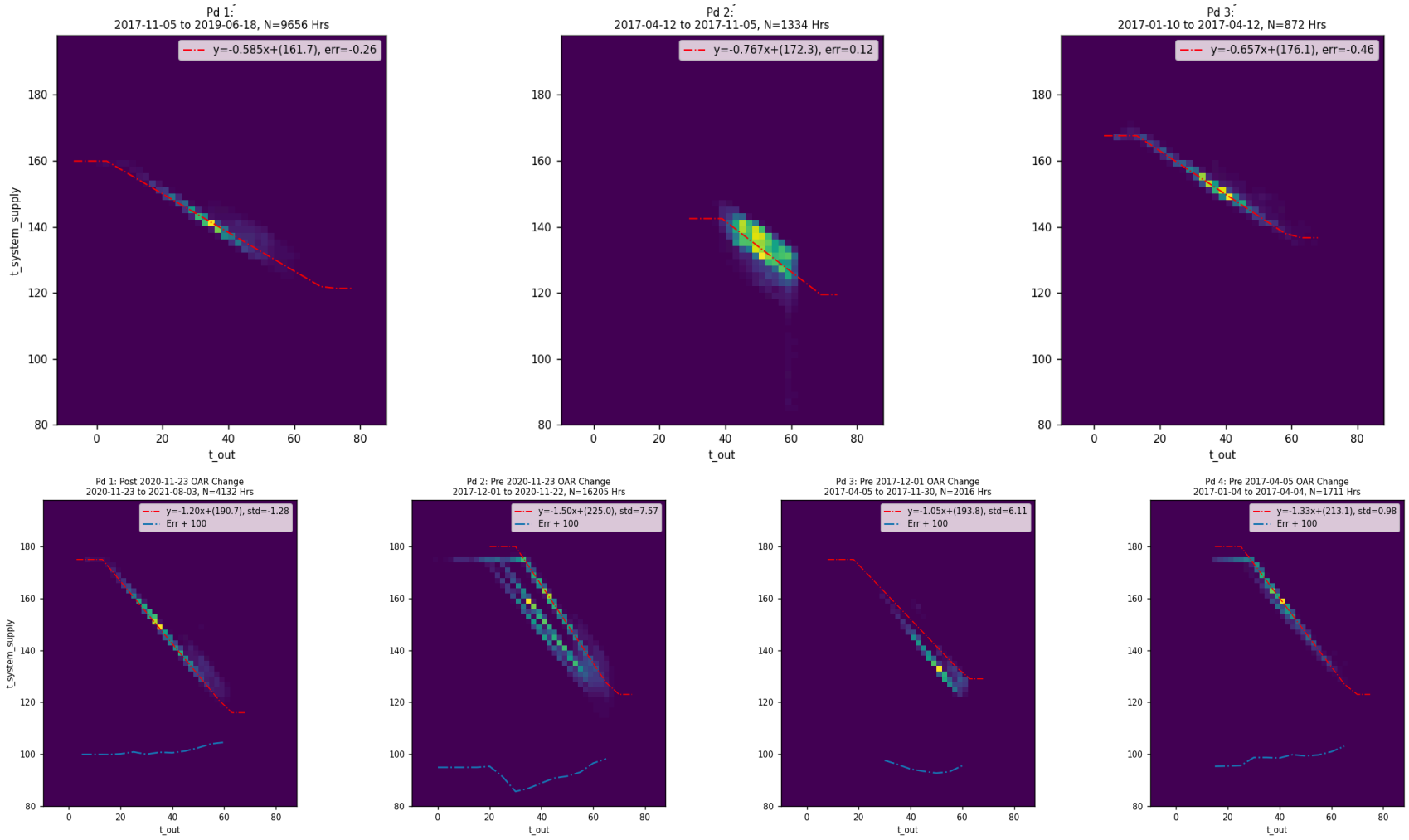

Figure 12: Example heatmap data visualizations for a plant with derived curves (top row) and configured curves (bottom row). For the configured curve case, note that the second (Pd 2) plot appears to capture multiple OAR curves. For the derived curve case, note that Pd 2 covers only a narrow range of outdoor air temperature (data goes from April through November), so there is insufficient data to derive an accurate curve across the plant's full operating envelope

3. Inactive or misconfigured warm weather shutdown (WWSD) and/or Summer-Winter Switch ("WWSD/SW-Switch")

When T_{out} exceeds a building's balance temperature, boiler space heating can usually be turned off to eliminate standby losses in boilers serving only space heating. Similarly, many jurisdictions specify times of year when landlords must provide heat, e.g., September 15th through June 15th in Boston, enabling the lock out of space heating outside that window. The tool analyzes boiler operations to meet space-heating loads and determines the extent to which they occur at warmer T_{out} or outside the heating season. The user can configure parameters to restrict analysis to different subsets of data and/or modify the data displayed.

This module analyzes the extent to which the heating system in a heating plant or combination plant operates at warm temperatures, and the extent to which the system operates during the non-heating season. At a minimum, it requires OAT and HTWS to execute, but performance is constrained if firing rate data is unavailable, and in the case of combination plants, if HWS is unavailable.

If firing rate data is available, the WWSD tool also estimates of potential savings for two defined WWSD thresholds, by default set to WWSD=62°F and WWSD=68°F. While this estimate provides a useful first order approximation, the estimate has several issues: (1) it is generated in isolation from other plant performance characteristics, and (2) data is not normalized to TMY conditions. The energy savings analysis generated downstream of the OAR analysis provides a more accurate, holistic estimate of potential energy savings from implementing this ECM; it also generates energy savings estimates only for Group H1 plants (heating plants w/firing rate data).[11]

WWSD analysis uses plant state estimation to demarcate periods when only the heating plant is active:

- For heating plants with firing rate data (Group H1 plants), this corresponds to periods with non-zero firing rate
- For combination plants, the WWSD tool treats time steps that are identified as heating-only calls as "heating active"; time steps that are identified as DHW calls or plant-off are treated as "heating off". Note that if HWS data is not available, DHW calls will be conflated with heating calls.

11 There are three specific issues with the WWSD savings estimate generated by this tool: (1) it does not account for the impact of inaccurate temperature sensor readings due to suboptimal sensor placement. This may mischaracterize the plant's control logic. This issue is addressed in the cross-cutting energy savings analysis tool. (2) When combined with other ECMs, savings are not necessarily additive: e.g., the energy savings impact estimated from implementing a lower WWSD and modifying OAR curve operating points may be higher when these measures are analyzed in isolation. The cross-cutting energy savings analysis tool calculates the integrated impact of ECMs; (3) The WWSD tool does not have the ability to model the impact of implementing a WWSD differential.

- For combination or heating plants without firing rate data, it is challenging to precisely characterize runtimes, so the WWSD/S-W Switch script adopts a different methodology for analyzing and visualizing plant data.

Methodology and results for plants with and without firing rate data are described below.

The WWSD/S-W Switch script outputs a table summarizing performance across all sites () and a series of plots providing visualizations for all sites or a subset of sites, depending on how the "show_all_plots" parameter is configured (). The WWSD/S-W Switch table includes the following metrics:

1. **PctOn-65-70Deg**: % of samples for T_{out} between 65-70 degree where heating operation is on. (flags if >10% samples are on)
2. **PctOn-70-75Deg**: % of samples for T_{out} between 70-75 degree where heating system is on (flags if >5% are on)
3. **PctOn-Summer, PctofSummersHrsOn**: % of samples and % of hours operational during non-heating season. Raises a flag if there are **any** instances of system operation.
4. **PctSavings-GT<XX>, PctSavings-SWSwitch:** Estimated savings if plant implemented WWSD at the two defined WWSD temperatures, and if S-W switch were implemented. WWSD estimates are generated by assuming that plant energy above the WWSD is zero post ECM; S-W switch estimates are generated by assuming that heating plant energy consumed between June 15th and Sept 15th is 0.

Site	PlantType	FirstReading	LastReading	SummerHrs	PctOn-65-70Deg	PctOn-70-75Deg	PctOn-Summer	PctOfSummerHrsOn	PctSavings-GT62	PctSavings-GT68	PctSavings-SWSwitch
102	heating	2021-04-16	2022-05-21	206	29%	20%	0.0%	0.0%	7.0%	1.6%	0.0%
13	combined	2017-01-04	2020-03-11	6476	4%	2%	2.0%	14.6%	nan%	nan%	nan%
8	combined	2017-01-03	2020-02-06	4922	1%	0%	0.2%	1.1%	nan%	nan%	nan%
9	heating	2017-01-04	2021-02-19	4572	23%	20%	19.8%	57.7%	9.3%	5.6%	5.6%
106	heating	2021-04-19	2022-05-25	1067	0%	0%	0.0%	0.0%	0.1%	0.0%	0.0%
167	heating	2021-04-19	2022-05-25	1067	0%	0%	0.0%	0.0%	0.1%	0.0%	0.0%
121	combined	2017-01-03	2022-05-21	3955	4%	2%	0.1%	0.9%	5.1%	1.2%	0.3%
27	combined	2017-03-09	2019-08-20	5535	9%	7%	1.8%	6.2%	nan%	nan%	nan%
181	heating	2021-11-23	2022-05-25	0	2%	2%	0.0%	0.0%	nan%	nan%	nan%
3	combined	2020-09-10	2021-06-28	330	8%	5%	0.0%	0.3%	nan%	nan%	nan%
7	combined	2017-01-10	2020-02-06	3662	3%	1%	1.2%	16.8%	5.2%	1.3%	2.0%
176	heating	2021-12-01	2022-05-25	0	0%	0%	0.0%	0.0%	nan%	nan%	nan%
177	heating	2021-12-01	2022-05-25	0	0%	0%	0.0%	0.0%	nan%	nan%	nan%

Figure 13: Example WWSD/SW Switch Summary table

If firing rate data is available, the WWSD/SW Switch script generates the following plots:

Scatter plot of the average heating system hourly duty cycle as a function of outdoor temperature

- Heatmap of the average heating system hourly duty cycle as a function of outdoor temperature
- A time series of heating system duty cycle overlaid with a plot of the summer shutdown period

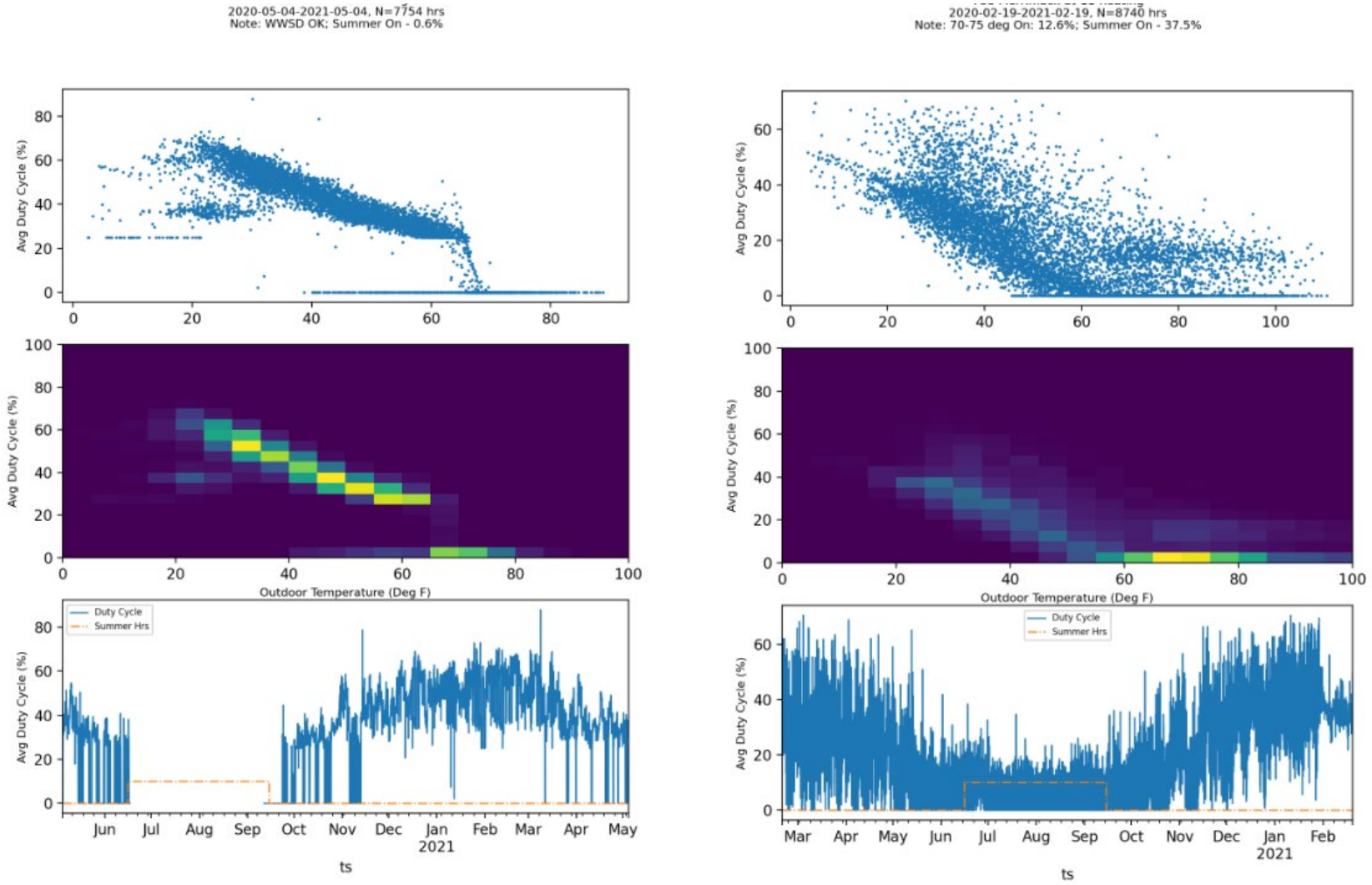

Figure 14: WWSD/SW Switch example plots for two different sites

Figure 14 shows example plots for two different sites. The left-hand plot shows data for a site that is performing as expected. In this case, the heating system operation shuts down above ~65 degrees and is largely inactive during the summer months (see e.g., the third plot of). The right-hand plot shows data for a site that is not performing as expected. As shown, the heating system is operational throughout the year, regardless of outdoor temperature or calendar.

For plants without firing rate data (Group H2 or C2 plants), plant state ("heating only on", "active dhw call", or "plant off") is determined by identifying periods with a rising supply temperature. This temperature-based state estimation presents two complications with respect to WWSD analysis:

1. The state estimation does not characterize heating system modulation: the plant state is either marked in an active state, or an off state.
2. Temperature-based state estimation does not accurately measure heating system runtime in cases where there is not measurable cycling of the supply temperature. During warmer months, in which heating system calls are typically short and infrequent, this may not be an issue; however, some plants exhibit minimal HTWS cycling during cold weather conditions, presumably because the heating plant is on nearly 100% of the time, and changes in modulation rate are not necessarily accompanied by measurable step changes in the supply temperature.

For plants without firing rate data, the state estimation tool addresses this lack of cycling during heating season using the following work-around: The heating system is marked as "active" every 30 minutes if the outdoor air temperature is less than 60 degrees and if there is no cycling observed within that window. Said another way, heating calls are defined by EITHER a sustained supply temperature rise OR (outdoor temperature < 60 degrees AND >30 minutes since reasonable subset of plant operating points where the heating system is active across a range of outdoor temperature conditions. However, this approach is not useful for characterizing the plant's duty cycle as a function of temperature.

As such, if firing rate is not available, rather than characterizing "duty cycle", the tool approximates the number of hours that the heating system is active per day as a function of outdoor temperature.

Sample plots for H2 and C2 plants are shown in . In this case, the y-axis represents hours per day when the heating plant is active. While this does not precisely measure duty-cycle, it does provide an effective means of identifying plants that appear to be active during summer months (e.g., in the example shown, the left-hand plot appears to have an effective WWSD, while the right-hand plot shows extensive warm-weather operation).

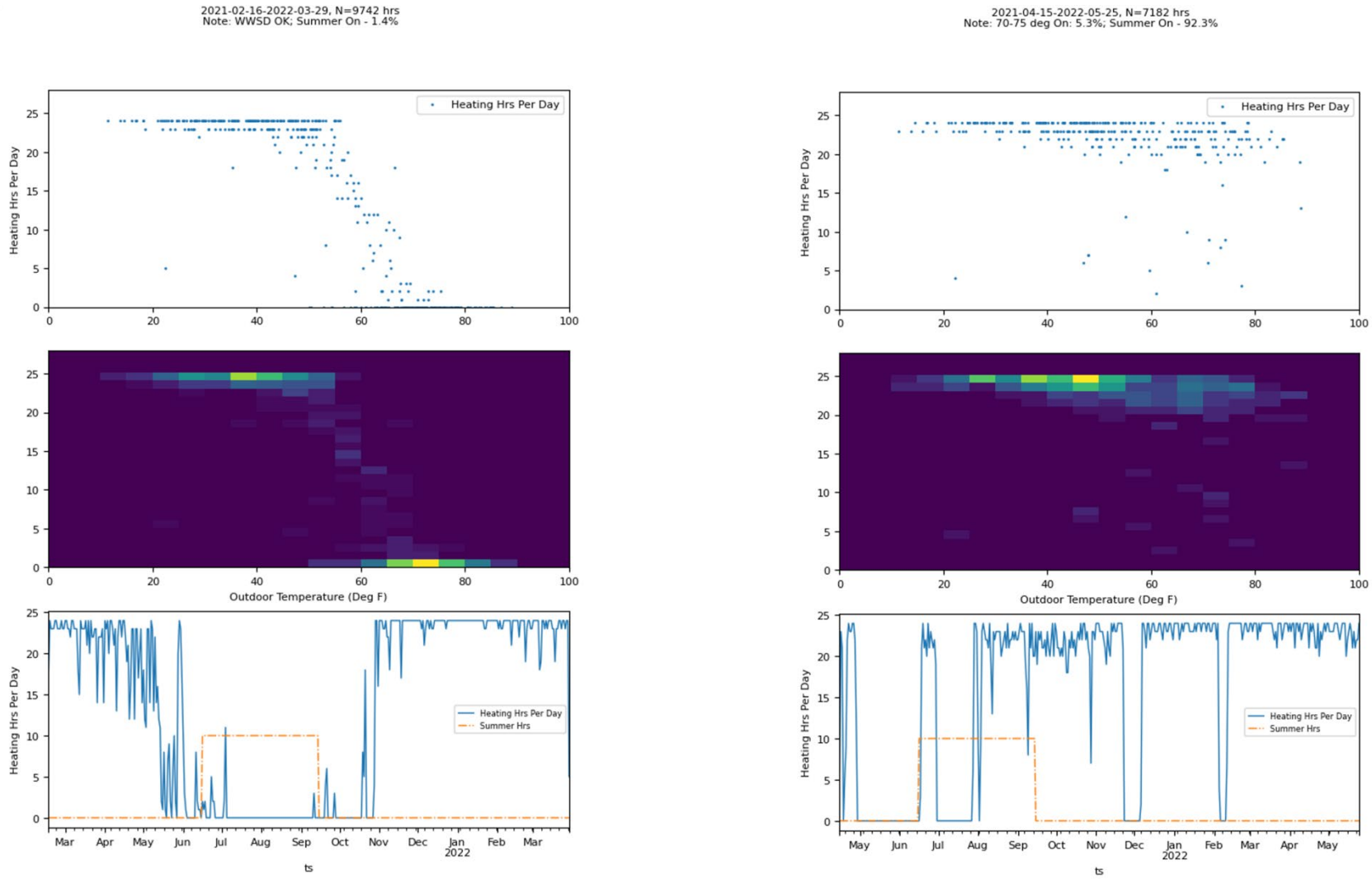

Figure 15: WWSD analysis for two sites. The left-hand site appears to be functioning near-optimally, as indicated by minimal operation during summer months and a linear drop in heating system hours at rising temperature, with minimal operation about 65 degrees; the right-hand site appears to have a significant issue with warm weather operation

4. Excess Boiler Cycling ("Excess Cycling")

Excessive boiler cycling increases boiler wear and wastes energy by increasing the number of boiler air-purge cycles. The tool analyzes how frequently the boiler operates in a "high cycle regime" (not necessarily a fault on its own) and the extent to which the heating system modulates its output within a high cycle regime. Lack of modulation coupled with high cycling often indicates excessive cycling that can be remediated by modifying boiler control parameters.

The boiler cycling analysis script generates a summary table (Figure 16) that includes the following metrics:

- **% High Cycle Hrs", # High Cycle Hrs:** A "high cycle hour" is defined as an hour with 5 or more boiler cycles. A "boiler cycle" is defined as an event in which firing rate goes above 1% and then drops below 1%. Currently does not support analysis for sites without firing rate, but this is in the pipeline.
- **LowLoad%:** Percentage of high cycle hours in which the firing rate is <=30%. If there are no "high cycle" hours in the data set, LowLoad% = nan. Raises a flag if LowLoad% > 40%.
- **HighLoad%:** Percentage of high cycle hours in which the firing rate is >=90%. If there are no "high cycle" hours in the data set, HighLoad% = nan. Raises a flag if HighLoad% > 40%.

Site	% High Cycle Hrs	# Hgh Cycle Hrs	LowLoad%	HghLoad%
29	2%	614	59%	1%
30	0%	3	nan%	nan%
34	22%	3041	4%	9%
35	9%	2287	47%	7%
7	0%	5	nan%	nan%
9	1%	520	99%	0%
20	0%	0	nan%	nan%
2	0%	0	nan%	nan%
22	0%	0	nan%	nan%
24	28%	4953	63%	1%
25	0%	0	nan%	nan%
11	8%	2454	90%	2%

Figure 16: Example excess cycling table

The boiler cycling analysis script also generates a matrix of plots for each site (Figure 17):

- The first row shows histograms of firing rate (column 1) and turn-ons per hour (column 2). This gets displayed for all sites, regardless of the prevalence of high-cycle regimes.
- The final row shows turn-ons per hour as a function of firing rate

If more than 100 "high cycle" hours (defined as >=5 turn-ons per hour, as defined above) are detected, two additional rows of plots are shown:

- The second row of plots shows the same two plots, but only includes high-cycle regimes.
- The third row shows average turn-ons per hour and a histogram of high-cycle events, both as a function of OAT.

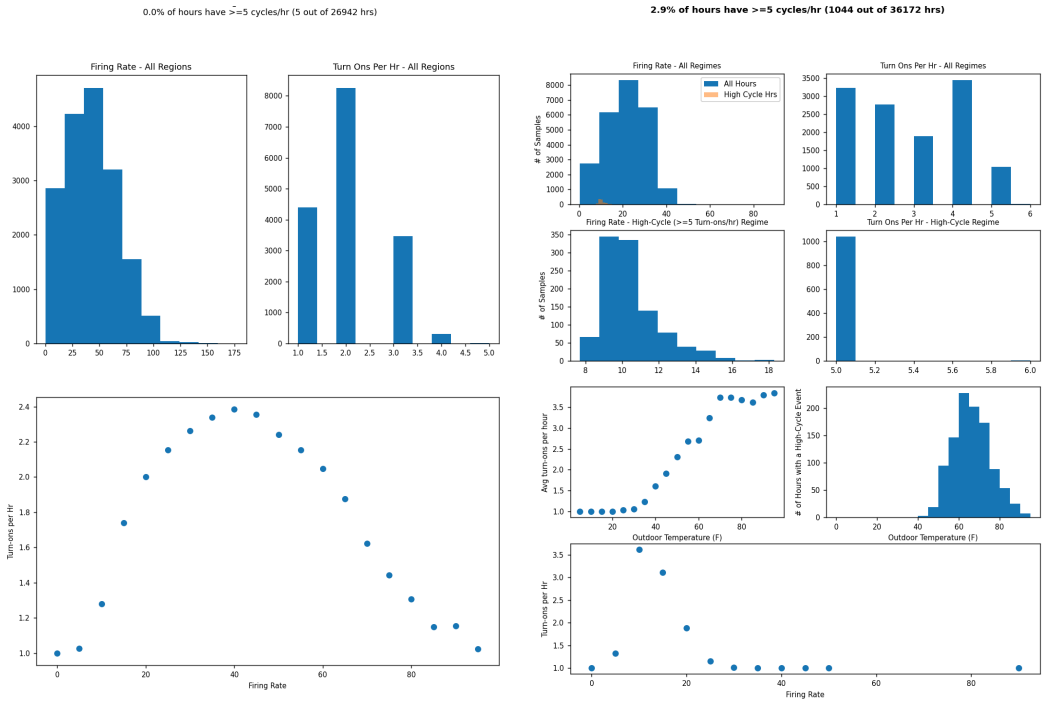

Figure 17: Example plots for two different sites; left hand site was not flagged; right-hand site was flagged for presence of high-cycle operating regimes.

This FDD Tool module also includes an analysis of the heating plant duty cycle as a function of OAT. This script plots either total Qin (*use_firing_rate=False*) or total firing rate (*use_firing_rate=True*) as a function of outdoor air temperature, with data averaged over several different timescales (Figure 18). Similar data is shown in tabular form (Figure 19).

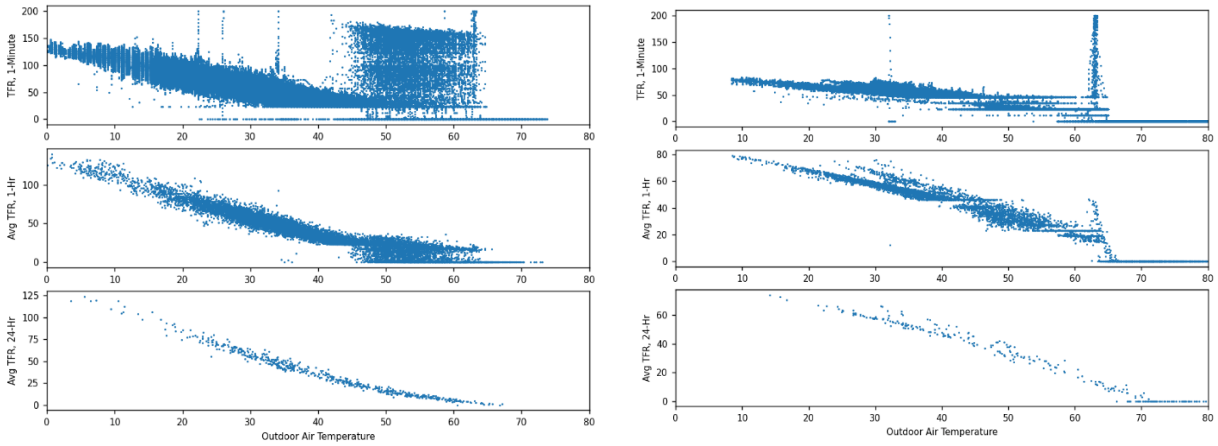

Figure 18: Total firing rate as a function of outdoor air temperature for two different sites. Data is shown over three different time-scales (1-min, 1-hr, 24-hr)

	Avg TFR, All Data	Avg TFR, ON Only	TFR>=50%	Tot Samples	Tot Sample w/TFR>50%
0	nan	nan	nan%	0	0
5	nan	nan	nan%	0	0
10	114.8	114.8	96.7%	30	29
15	111.4	111.4	83.6%	1635	1367
20	108.6	108.6	81.4%	7054	5739
25	99.0	99.0	86.1%	9661	8318
30	91.1	91.1	85.9%	15504	13320
35	82.5	82.5	84.5%	14108	11917
40	70.7	70.7	83.9%	16220	13606
45	62.3	62.3	73.5%	14562	10705
50	53.9	53.9	49.4%	9521	4700
55	47.0	47.0	32.4%	4296	1394
60	39.0	39.0	4.9%	3576	174
65	25.0	40.4	10.2%	1124	115
70	0.0	nan	nan%	0	0
75	0.0	nan	nan%	0	0
80	nan	nan	nan%	0	0
85	nan	nan	nan%	0	0
90	nan	nan	nan%	0	0
95	nan	nan	nan%	0	0

Figure 19: Total firing rate (TFR) and TFR > 50% as a function of outdoor air temperature.

shows boiler firing rate (summed across all boilers) as a function of outdoor air temperature for two different sites (left and right plots). At both sites, at moderate temperatures (e.g., 40-55 deg), the plant runs at approximately steady state at a 20-30% modulation level. However, at higher temperature (>55 degrees), if on, the firing rate is often near full load. To be clear, the average duty cycle, when averaged over 1-hour or 24-hour periods, is reasonable given the outdoor temperature condition – but when the plant cycles on, it cycles on to full power. This type of behavior can indicate potential for one of a few ECMs. The site on the left is indicative of a plant that is unable to modulate low enough to serve its heating load, so it cycles on and off

at full power over a relatively wide temperature range; this could indicate that the boiler is over-sized for this site, or that it's a good candidate for a hybrid heat pump system. The right-hand plot likely shows full-power cycling over a relatively narrow temperature band. This indicates the plant is likely coming out of warm weather shutdown and tries to raise the supply temperature as rapidly as possible. This could potentially be accomplished more efficiently by operating the boiler at a lower firing rate.

5. Misconfigured DHW setpoints ("DHW Setpoint")

The DHW Setpoint Analysis module implements three fault detection algorithms:

- *Low Domestic Hot Water Storage Temperature (HW):* Identifies DHW systems with low DHW storage temperatures, which can pose a *legionella* risk.
- *High DHWS:* Detects high DHW Supply temperatures (DHWS) that could pose a scald risk and/or increase pipe heat losses.
- *DHWS-DHWR Differential Out-of-Range*: The relationship between DHWR and DHWS can help uncover multiple faults, including recirculation pump reversal or frozen/failed mixing valve (see DHW Fault documentation for additional discussion).

This toolset analyzes data from DHW plants or from combination plants, and polls data from DHWS, DHWR, HW, and tank setpoint, but it will execute with any combination of these endpoints available, albeit with reduced scope.

Tank setpoint data is not used for fault detection, rather HW is used as a proxy for in-tank conditions. The logic for using HW in lieu of tank setpoint is that (a) it provides a measure of actual water temperature; and (b) it does not require data collected via MODBUS or other BMS protocols.

If HW data is not available, it is assumed that the site does not have a mixing valve.

The following default parameters are used but can be changed by the end-user.

Table 2: DHW fault identification parameters

Name	Description	Value
tank_setpoint_low	HW Threshold to flag for low setpoint	140
dhw_setpoint_low	DHWS threshold to flag for low setpoint	112
tank_setpoint_high	HW Threshold to flag for high setpoint	140

dhws_setpoint_high	DHWS threshold to flag for high setpoint	130
dhws_rev_err_thresh	Threshold above which to flag DHWR > DHWS	0.10

Note: Although tank_setpoint_low and tank_setpoint_high are configured to the same value, the criteria for flagging these faults differ.

The time window for analysis, e.g., to see when changes may have occurred, may be configured in two different ways:

- If "lookback_days" is set to a value other than "None", the analysis runs from lookback_days before the site's most recent data point to the most recent data point.
- If lookback_days is set to "None", the time window is bracketed by *st* and *et* (start and end times)
  - If *st* is set to "None", start time is the first data point for the site
  - If *et* is set to "None", end time is the most recent data point for the site

For each DHW plant, the DHW fault assessment tool (a) displays several data visualizations for each site to provide supporting context; and (b) checks observed operation relative to pre-defined set points to identify possible fault conditions. The tool presents results of fault screens in a summary table (Figure 20), along with supporting data.

	DHWS / DHWRErr	Pct DHWR> DHWS	LowSetPtErr	HW-Min, Daily Max	DHWS-Min, Daily Max	tank_setpoint-Most Recent Val	PctDays	ScaldRiskErr	90th% DHWS	MixValveErr	10th% DHWS	HighSetPtErr	10th% HW
Site 1-dhw	False	3.4%	True	139	131	nan	26.0%	True	139	False	119	False	132
Site 2-dhw	False	0.6%	True	136	135	133	95.4%	True	138	True	130	False	135
Site 3-dhw	False	0.4%	True	131	124	132	88.0%	False	130	True	122	False	130
Site 4-dhw	False	0.6%	True	138	124	nan	85.7%	True	133	True	128	False	136
Site 5-dhw	True	15.7%	False	nan	135	132	0.0%	True	137	False	120	False	nan
Site 6-dhw	False	2.0%	True	130	127	119	87.5%	False	128	False	114	False	126
Site 7-dhw	False	0.3%	True	134	129	134	90.6%	True	136	True	128	False	132
Site 8-dhw	False	0.0%	True	127	126	118	73.6%	False	126	False	119	False	120
Site 9-dhw	False	0.1%	True	120	121	nan	92.1%	True	138	False	119	False	128

Figure 20: DHW Fault Summary output table

identifies the following fault conditions:

"**DHWR/DHWSErr" –** Indicates possible recirculation pump reversal or mixing valve issue. This flag is raised if DHWR > DHWS for more than 10% of samples.

> Supporting data: "Pct DHWR>DHWS" column shows the actual percentage. If nan appears, it indicates that one or more required data point is missing.

"LowSetPtErr" – Indicates risk of *legionella* bacteria growth. This flag is raised if more than 1% of days analyzed have a maximum HW < 140°F or maximum DHWS < 112°F.

Supporting data:

- 1st percentile values for the daily max value of HW and DHWS ("HW-Min, Daily Max", "DHWS-Min, Daily Max")
- The most recent tank temperature set-point value;
- The percentage of days on which either the max HW or the max DHWS value was below the relevant threshold

"ScaldRiskErr" – Indicates potential scalding risk due to excessive DHWS temperature. Flag is raised if more than 10% of DHWS sensor measurements exceed 130°F.

Supporting data: 90th percentile DHWS shows the 90th percentile value for DHWS. If >130°F, flag is raised.

"HighSetptErr" – Indicates potential to decrease DHW tank temperature set point to optimize system energy use:

- For sites with a HW measurement: Raises a flag if >90% of HW measurements > 140°F
- For sites with no HW measurement, indicating no mixing valve, a HighSetptErr flag occurs if >90% of DHWS measurement exceed 122 °F (low end of acceptable DHWS range + 10°F).

"MixValveErr" – Indicates potential DHW mixing valve fault or high DHWS set point setting. Raises a flag if a system has a mixing valve (i.e, HW is present) and >90% of DHWS measurements >122°F (low setpoint + 10 degrees).

DHW Data Visualization

Two to three plots are generated for each site as seen in Figure 21. The third plot is generated only if an error is detected. Note that the plot title summarizes results of the fault identification screen.

- **Plot 1 -** Time-series of the **daily maximum** value of HW, DHWS, and Tank Setpoint, as available.
- **Plot 2 -** A box and whisker plot showing the range of values for (1) *Daily Max* HW and DHWS (used to identify low set-point faults) and (2) *All* HW and DHWS data points (used to evaluate high set-point faults and scald risk) . The box boundaries represent the 25th and 75th percentile values; the whiskers represent the 5th and 95th percentile values.
- **Plot 3 –** A box and whisker plot to illustrate relationship between DHWS and DHWR. The relationship between DHWR and DHWS helps identify multiple faults, including recirculation pump reversal or a mixing valve issue. The tool only displays this figure if a fault is detected (i.e., DHWR > DHWS for more than 10% of samples).

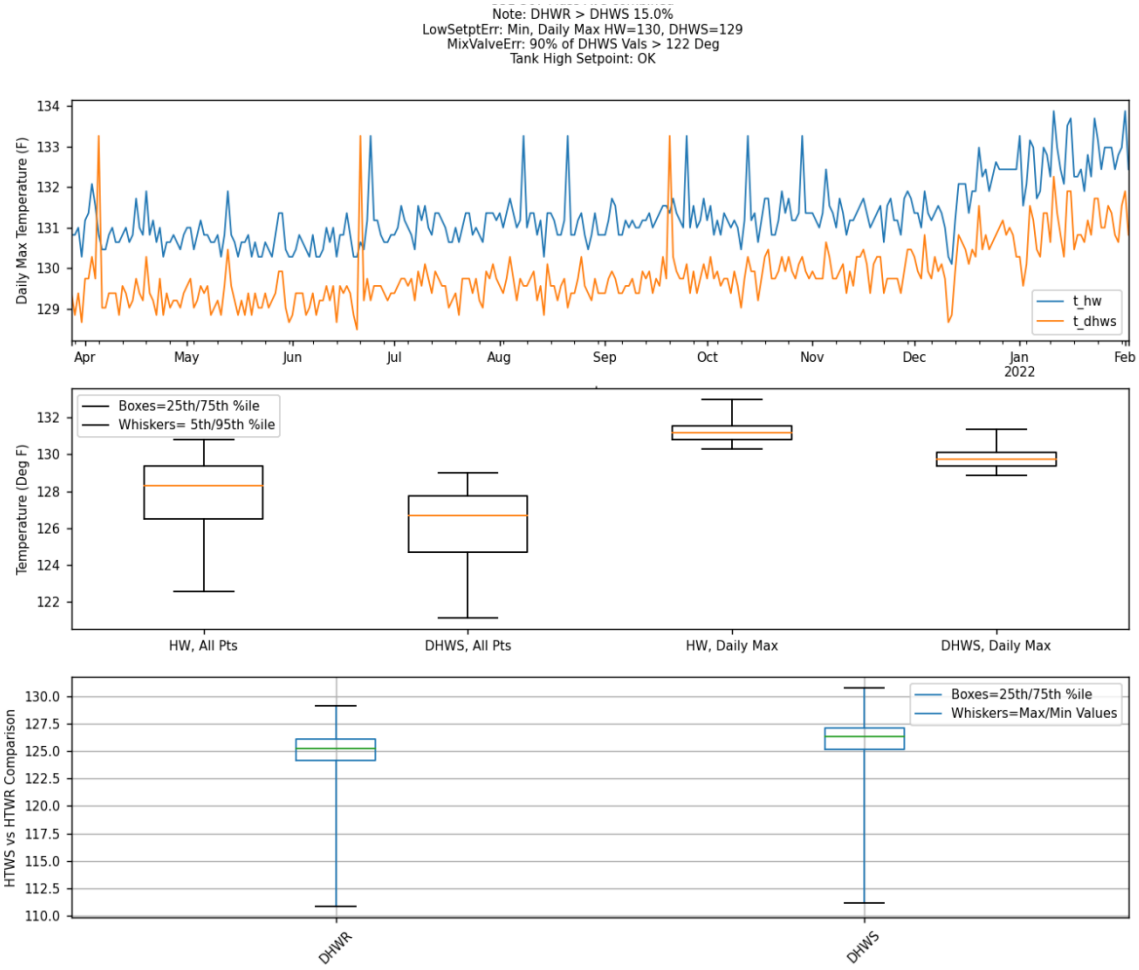

Figure 21: DHW fault detection data visualization

The tool also generates a table (see Figure 22) showing statistical distributions of the "daily max" values, with color coding indicating whether a data point is above/below the "LowSetptErr" threshold (112ºF for DHWS, 140ºF for HW).

	HW-1%	HW-25%	HW-50%	HW-75%	HW-99%	DHWS-1%	DHWS-25%	DHWS-50%	DHWS-75%	DHWS-99%
Site 1-dhw	139	142	143	144	154	131	140	141	143	146
Site 2-dhw	136	139	139	140	148	135	137	138	139	145
Site 3-dhw	131	138	139	139	148	124	133	135	136	138
Site 4-dhw	138	139	139	139	140	124	133	133	134	136
Site 5-dhw	nan	nan	nan	nan	nan	135	136	138	140	145
Site 6-dhw	130	132	132	133	134	127	128	129	129	131
Site 7-dhw	134	135	136	143	148	129	131	133	135	143
Site 8-dhw	127	128	128	128	129	126	127	127	127	134
Site 9-dhw	120	138	139	140	144	121	133	139	140	141

Figure 22: DHW analysis – statistical distribution report output table

Quantification of Energy Savings from ECM Implementation

Prior Energy Savings Estimates: NEI's prior work on >100 multifamily buildings in Massachusetts[12] resulted in more than 80% of the sites realizing energy savings from remote monitoring and optimization, with those 80% realizing an average savings of 11% based on pre-/post- utility bill analyses. Since that was the first iteration of implementing changes in the field, NEI generally had taken a more conservative approach to potential controls modifications to minimize potential complaint calls until it better understood how changes affected system performance.

Modeled Energy Savings Estimates: As described in the Boiler Efficiency document submitted to DOE during BP1, the tool uses engineering models to estimate energy consumption for baseline and post-ECM cases. First, the tool analyzes existing boiler performance data to derive additional variables used in the physics-based models to characterize system energy performance, such as boiler inlet temperatures as a function of T_{out}. With these models established, the tool then exercises the model for a typical mean year (TMY3) of weather data for both the baseline and ECM cases, where the ECM case includes changes to physical parameters (e.g., OAR curve parameters, (which, in turn, affect boiler efficiency), and when

12 This pilot project was funded by the Massachusetts Clean Energy Center (MassCEC). As such data from these buildings may be referred to as MassCEC sites.

boilers are allowed to fire (WWSD temperatures, W-S lock-out dates)[13]. The difference between the two cases equals the expected energy savings, assuming no other substantive changes.

Updated OAR-Driven Energy Savings Model: The initial implementation of the energy savings described above modeled OAR-driven savings as a function of boiler efficiency while assuming that the building's underlying heat load remains unchanged. Such a model would apply for a building with perfectly controlled heat flow into the building. A subsequent iteration sought quantified the effect of building overheating due to, for example, failed thermostatic valves (TV) that would result in uncontrolled heat flow into the building. The magnitude of the losses associated with uncontrolled heat flow varies considerably as a function of the differential between the HTWS and outdoor temperature, so modifying HTWS set points can have a sizeable impact on building heat load. Our initial implementation of the building loss model assumed fully controlled heat flow case (0% of TVs failed, i.e., best-case condition), and therefore systematically under-estimated savings.

In practice, OAR-driven savings should fall somewhere between the controlled and uncontrolled cases. The updated revision compares observed energy consumption relative to that predicted by the controlled and uncontrolled cases to determine where along the continuum from "fully controlled" to "fully uncontrolled" the system resides.

Integration of downstream impact of T_{out} *error + composite savings estimates:* Updates account for the integrated impact of OAR curve modifications, warm weather shutdown (WWSD) set point modifications, and remediation of temperature sensor placement.

Updated ECM Data Model: Ingests an Excel configuration file that specifies combinations of ECMs (OAR settings, WWSD settings, and temperature sensor placement) to evaluate the impact of remediation.

Comparison of ECMs Identified Manually and by the Tool

To evaluate the performance of the tool relative to manual analysis, an NEI analyst applied the tool to 19 sites to determine if the targeted faults existed. For each site, the analyst compiled the following information:

- Faults identified by the tool and manual analysis;
- Faults identified by the tool, not by manual analysis;
- Faults not identified by the tool, identified by manual analysis, and
- Time to complete analysis using the tool.

13 Handling changes in Tout sensor placement is more involved, as described in the documentation submitted to DOE.

We then analyzed those outcomes, deriving the information summarized in and below. In some cases, the analyst was not able to come to a yes-no decision as to whether a fault exists, while in others the tool lacked sufficient data to perform an analysis; both count as "skip."

	Analysis Faults Detected							FDD Tool Faults Detected						
Site	Suboptimal	No Tout	Suboptimal	Excessive	No	No S/W	High DHWS	Suboptimal	No Tout	Suboptimal	Excessive	No	No S/W	High DHWS
MassCEC Site 1	y	n	y	n	n	n		y	n	y	n	n	n	y
MassCEC Site 2	y	n	y	n	n	n	n	y	n	y	n	n	n	n
MassCEC Site 3	y	n	y	n	n	u	y		n	y	n	y	n	
MassCEC Site 4	y	n					y	y	n			n	y	y
MassCEC Site 5	y	n	y	n	n	n	n	y	n	y	y	n	n	n
MassCEC Site 6	y	n	y	u	y	n	n	y	y	y				n
MassCEC Site 7	y	n	u	y	y	n	y	y	n	y		n	n	y
MassCEC Site 8	y	n	y	y	y	y	y	y	n		y	y	y	n
MassCEC Site 9	y	n	y	y	n	n	y	y	n	y	y	n	n	y
MassCEC Site 10	y	n		y	y	y		y	n	n		n	n	y
MassCEC Site 11	y	n	y	n	n	n	y	y	n	n	n	n		y
MassCEC Site 12	y	n	y	u	n	n	y	y	n	y		n	n	y
MassCEC Site 13	y	n	y	y	n	y	y	y	n	y	y	n	y	y
MassCEC Site 14	y	n	y	n	n	y	y	y	n	y	y	y	y	y
MassCEC Site 15	y	n	y	y	n	n	n	y	n		n	n	n	y
MassCEC Site 16	y	n	u	u	n	n	n	y	n			n	y	y
MassCEC Site 17	y	n	y	n	n	n	y	y	n		n	n	n	
MassCEC Site 18	y	n	n	n	n	y	y	y	n		n	n	y	
MassCEC Site 19	y	n	y	n	n	y	y	y	n	y	n	n	y	

Figure 23: Summary of fault detected from manual analysis and the tool. Green equals agreement, gold disagreement, and yellow/peach unclear

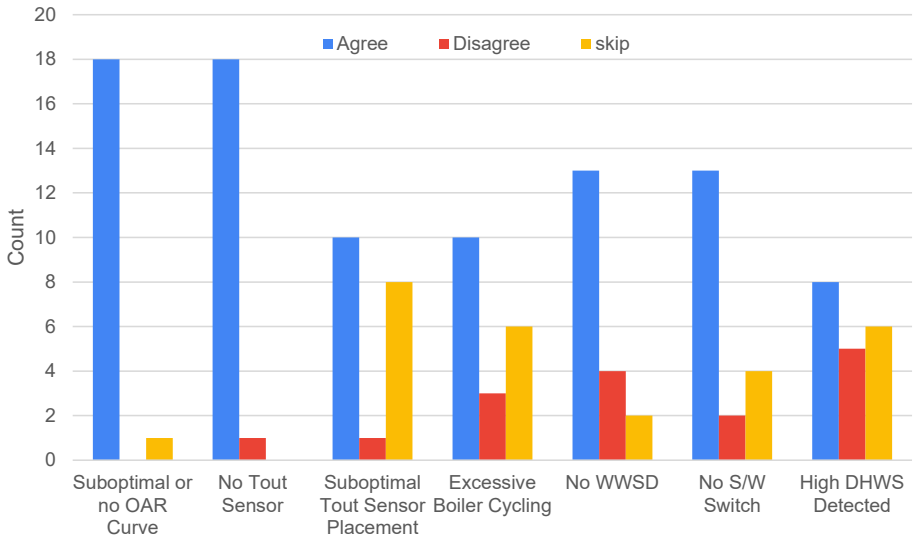

Figure 24: Alpha tool classification accuracy

Overall, the tool and the prior evaluation agreed on 85% of the assessments (excluding skips), with the highest agreement found for Suboptimal/No OAR Curve and T_{out} Sensor faults.

Eliminating the less-mature High DHWS fault, 88% of non-skipped assessments agreed.[14] In general, we selected thresholds for faults that tend to flag sites for further investigation by the analyst if the data suggest that a fault may exist; consequently, we likely flag more false positives than if the tool were trying to yield the highest classification accuracy. In testing, false positives accounted for half of the disagreements between the tool and prior evaluations.

Objective 2: Reduce analysis time by 80%+ relative to manual approaches

NEI used a manual process to analyze data from monitored sites during its MassCEC project comprising >100 sites, reviewing data in SkySpark and entering key data points into a spreadsheet for evaluation. Although this process successfully identified the key faults discussed earlier, NEI found that

- Manual analysis processes, the first of three steps to deliver an ECM, consumed an average of three (3) hours per site. This includes the time spent for data quality control (QC), to conduct the heating curve analysis and evaluate other potential faults, incurred each time a site is analyzed.
- The second step of specifying a new heating curve and DHW settings required about one hour.
- The final step of ECM completion, including identification of needed repairs, the implementation steps specific to the site and overall QC, takes about six (6) more hours. In total, the current processes take a total of about 10 hours/site, down from the 16-20 hours/site indicated in the proposal.

Using a locally stored file, a full site analysis comprising data QC and fault evaluation takes about three minutes on a laptop computer. The tool can run these analyses overnight or while the analyst completes other activities, meaning that the analysis primarily spends time reviewing the summary findings and associated plots and tables generated, evaluating data issues or unclear performance issues flagged, and deciding what ECMs and fixes to recommend to different property managers. Because the analyst can run the tool in the "background" with minimal effort, site analyses can be performed much more frequently than before (e.g., monthly versus once) for portfolios of sites, increasing the value of the tool and the energy savings realized (since suboptimal operations are flagged sooner).

- FDD tool enables more savings by being able to run quickly/more often. Savings are constantly under attack of overrides
- Identifying overrides closer to when they happen, and quickly identifying the date/time they happened allow for the most informed conversations with site staff, rather than thinking back further into the past. This increases trust, allows identification of other

[14] This analysis was completed using an earlier Alpha version of the FDD tool. Because there was insufficient time to repeat this analysis with later versions, it is worth noting that this may not represent the tool's full capabilities.

issues within the building that can be fixed, and reinforces the benefit of having the monitoring more often.

- Identifying the time frame where changes happen is a new feature which doesn't exist within our manual analysis tool without iterations by the user

The NEI analyst recorded the time it took to run complete analyses with the tool to analyze the performance of 19 existing buildings (see earlier discussion of Objective 1). On average, an analysis of a batch of five sites took about:

- 10 minutes to configure and run the tool
- 40 minutes to review the tool outputs.
- or about 10 minutes per site.[15]

This represents a 94% reduction from the three hours required for the manual approach, exceeding our 80% reduction goal.

Objective 3: Calculate weather-adjusted energy savings estimates that will be within ±20% of achieved energy savings, based on pre-ECM and post-ECM gas consumption data.

As described in the discussion of Objective 1, we have developed a simple physics-based model that uses connected boiler system data to characterize the extent of overheating occurring in each building due to uncontrolled heat flow. The model also can be applied to predict the change annual space heating energy consumption from changes in OAR curve parameters.

To validate the model, we applied this methodology to 19 different OAR curve and WWSD changes made at 12 different sites in Massachusetts[16] with boiler systems monitored using New Ecology's Remote Monitoring & Optimization (ReMO) platform that acquired HTWS, HTWR, BFR, and T_{out} data (New Ecology 2023)[17]. For more detail on data acquisition, please see Davey and Connelly 2018 New Ecology 2018. To avoid confounding factors, we limited our analyses to sites where the boilers only served space heating loads, i.e., they did not serve water heating loads.[18] For both cohorts, data were divided into "pre" and "post" periods that correspond to

15 Similarly, end-to-end testing of the tool found that running and reviewing complete analyses for three sites took a total of 20 minutes.

16 Located mainly – but not all – in Greater Boston, the sites included masonry, concrete, and wood-frame buildings constructed between 1900 and 2002 with 15 to >150 units on three to 16 stories. Each building had at least two boiler that could serve space heating loads, with capacities ranging from a few to several hundred kBtuh.

17 The surface-mounted temperature sensors for HTWS and HTWR were both installed in the boiler room, with HTWS typically located immediately downstream the heating water distribution pump(s) and HTWR downstream of the piping manifold (if any) that combined separate heating water loop returns.

18 For boilers serving both space and water heating loads, we have developed data-driven techniques to disaggregate boiler energy consumption time series between space and water heating.

periods with different OAR curves. In all cases, we used the "pre" data to model the boiler plant and then apply the model to the "post" period actual weather to predict "post" period performance, ultimately comparing modeled (*predicted*) energy consumption to *actual* post-ECM energy consumption. Figure 25 below shows an example of multiple OAR curves derived from the connected boiler data (each data point shown is average temperature for an hour) for one site.

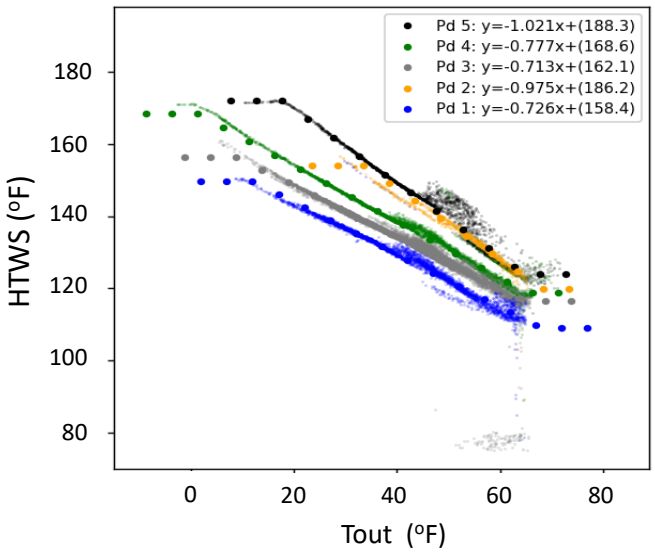

Figure 25: Example of five OAR curves derived from connected boiler data for site 1020. The small points represent hourly data, the larger points averages for 5°F T_{out} bins

Figure 26 presents pre and post hourly Qin data for another site, along with the ideal and uncontrolled curves for the pre and post OAR curves, as well as the average Q_{in} values (triangles) for the 5°F T_{out} bins.

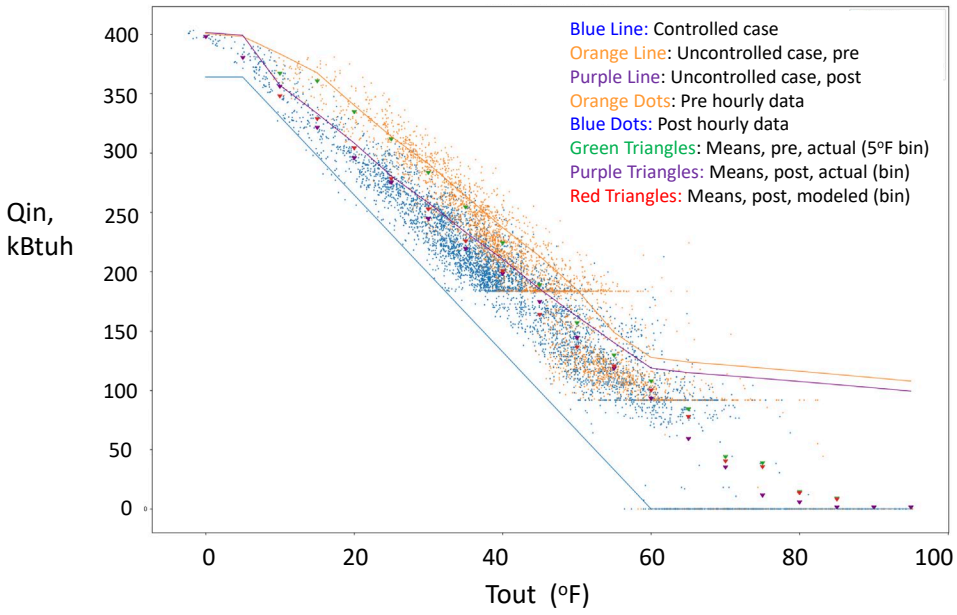

Figure 26: Example of Q_{in} analysis for site 1020, showing pre and post data relative to controlled and uncontrolled heat flow cases

Table 3 summarizes the OAR curve changes made to the boiler systems.

Table 3: OAR curve parameters for the 19 changes evaluated at 12 sites. Format is: T_{out} /HTWS,max to T_{out} /HTWS,min. All temperatures in ºF

	Period		WWSD	OAR Curve	
Site	*Pre*	*Post*	*Pre to Post*	*Pre*	*Post*
1020	2	0	65 to 65	8/156 to 64/117	12/150 to 68/109
1020	3	2	70 to 65	0/169 to 64/119	8/156 to 64/117
1020	4	3	70 to 70	16/172 to 63/124	0/169 to 64/119
1020	4	0	70 to 65	16/172 to 63/124	12/150 to 68/109
1007	1	0	83 to 75	10/180 to 70/120	10/170 to 65/115
1023	1	0	70 to 62	11/136 to 60/120	10/140 to 60/101
41	1	0	67 to 67	14/169 to 65/133	20/162 to 60/133
41	2	1	70 to 67	34/169 to 67/142	14/169 to 65/133
41	4	3	70 to 65	29/170 to 62/145	25/161 to 69/131

43	1	0	65 to 65	39/187 to 69/153	8/168 to 64/114
1009	1	0	67 to 62	33/175 to 68/123	14/175 to 60/119
1009	2	1	69 to 67	22/176 to 65 121	33/175 to 68/123
1009	4	3	67 to 67	31/175 to 64/115	18/175 to 68/111
1013	2	0	70 to 62	10/169 to 68/102	5/173 to 60/100
1028	1	0	70 to 65	10/163 to 60/109	25/166 to 60/135
55	2	1	65 to 61	39/151 to 67/138	14/170 to 60/115
1016	1	0	None	10/169 to 60/124	2/162 to 61/117
23	2	0	70 to 62	13/168 to 60/137	3/162 to 69/121
24	2	1	70 to 65	15/166 to 63/124	35/165 to 61/120

For the 19 different OAR changes, we modeled the expected energy savings using the following process:

- Analyze boiler data from the "pre" period to calculate hourly space heating energy consumption.
- Calculate the total boiler system gas input (HHV), $Q_{gas,in}$, for each hour by summing the product of boiler firing rate (BFR) and boiler capacity for all boilers.
- Estimate the average boiler efficiency for each boiler during each hour using a curve for η(HTWR,BFR) derived from Lochinvar (2019).
- Calculate the hourly Q_{in} = Qgas,in,pre * η(HTWR,BFR)
- Calculate the average Q_{in} for each 5°F T_{out} bin for the entire "pre" period
- Estimate $T_{out,design}$; since the boiler plants analyzed were in Boston, MA and vicinity, we used $T_{out,design}$ = 5°F.
- Estimate $Q_{in,design}$ from the hourly Q_{in} data in the vicinity of $T_{in,design}$.
- Calculate the $Q_{in,contr}$ and $Q_{in,uncontr}$ heat flow curves using the respective equations above.
- Calculate SC(T_{out}) for each 5°F T_{out} bin using the calculations described in Appendix C.

We then applied the SC(T_{out}) factors calculated for the "pre" period with the pre and post HTWS values (T_{out}), i.e., HTWS,new and HTWS,old, to calculate dQ_{in} (T_{out}) and, hence, the expected

post space heating load and gas consumption, Q_{in} ,post(T_{out}) and Qgas,in,post, taking into account the impact of OAR curve changes on both space heating loads and boiler efficiency. Finally, Q_{in} ,post(T_{out}) is applied to local TMY T_{out} data to calculate the total expected boiler energy consumption for the entire "post" period.[19] At all sites, we used the HTWS(T_{out}) curves derived from the field data instead of those specified for the "pre" and "post" periods.

For all sites, we calculated the following metrics:

- "Modeled Savings": Expected percent savings from OAR, WWSD, T_{out} sensor[20], and Summer-Winter Switch[21] based on TMY data.
- "Observed Savings": Actual savings observed, after applying adjustments to normalize bin frequency for pre- and post-ECM Q_{in} -vs-temperature, based on TMY data.

Table 4 and Figure 27 summarize the comparisons of the modeled (predicted) and observed (actual) savings. Although there is some scatter, the absolute values[22] of the modeled and observed savings are 12.8% and 11.3%, respectively, with an average absolute difference of 4.3%.[23] For the 19 changes, the model predicted actual savings within ±5% for 13 of them and within ±10% for 16 of them. Taken together, these results strongly suggests that the new approach effectively models the energy impact of overheating from boiler systems due to uncontrolled heat flows and the impact of changing HTWS(Tout) on boiler energy consumption.

Interestingly, there is not always a strong correlation between SC values and the magnitude of modeled savings. This reflects that the magnitude of changes to OAR curve parameters also has a large impact on expected savings, e.g., the three sites with modeled savings exceeding 20% had larger changes in the OAR curve parameters. In addition, we calculated savings based on the actual Tout conditions during the post period. That is, the post period may include warmer or colder conditions than TMY conditions, which can substantially affect the savings period for that period. Finally, the magnitude of WWSD changes – and their savings – varies appreciably. For these reasons, the typical annual savings from changing boiler control settings can vary

19 Since sites often implemented changes to WWSD measures, we also modeled their energy impact; see Appendix.
20 The Tout sensor was also moved at a few sites, which affects the Tout value used by the boiler system to determine HTWS(Tout); we took that into account.
21 A summer-winter switch (SWS) locks out space heating functionality for a boiler system during a set time of the year, e.g., mid-June through mid-September.
22 For cases with negative savings, typically due to an increase in OAR curve parameters, we calculated the absolute value of savings by effectively switching the pre and post case, i.e., savings = (% savings)/(1-% savings).
23 Ignoring the outlier for site 41, between periods 4 and 3, the modeled and expected savings are 12.9% and 10.9%, respectively, with an average absolute difference of 3.8%. At site 41, Tout during period 4 was very warm; as a result, the impact of heat gains not captured by the model on total space conditioning loads increases as conduction and infiltration loads driven by ~Tin-Tout decreases. Specifically, 48% of the post-ECM samples are >62.5 °F, i.e., a Tout regime with very large savings from both OAR changes and WWSD changes. In short, the post period is not very representative of the entire space heating season.

appreciably from those shown; our analyses focused on evaluating the accuracy of the algorithms.

Table 4: Summary of Modeled and Observed Savings for OAR Changes at Different Sites. Negative Numbers Represent an Increase in Energy Consumption

Site	*Pre*	*Post*	*Modeled*	*Observed*	*Difference*	*SC*
1020	2	0	10.8%	5.6%	5.2%	0.75
1020	3	2	9.5%	-1.4%	10.9%	0.77
1020	4	3	10.4%	11.7%	-1.3%	0.69
1020	4	0	16.9%	15.8%	1.1%	0.67
1007	1	0	11.1%	1.8%	9.3%	0.83
1023	1	0	12.4%	-1.8%	14.2%	0.33
41	1	0	5.3%	9.0%	-3.7%	0.59
41	2	1	22.5%	19.8%	2.7%	0.65
41	4	3	12.3%	24.6%	-12.3%	0.52
43	1	0	27.4%	27.3%	0.1%	0.18
1009	1	0	17.9%	12.9%	5.0%	0.57
1009	2	1	-8.9%	-2.1%	-6.8%	0.68
1009	4	3	2.7%	2.6%	0.1%	0.60
1013	2	0	9.2%	10.7%	-1.5%	0.82
1028	1	0	20.7%	23.7%	-3.0%	0.34
55	2	1	14.0%	16.0%	-2.0%	0.54
1016	1	0	8.1%	9.3%	-1.2%	0.32
23	2	0	10.1%	12.7%	-2.6%	0.65
24	2	1	-15.1%	-14.7%	-0.4%	0.68

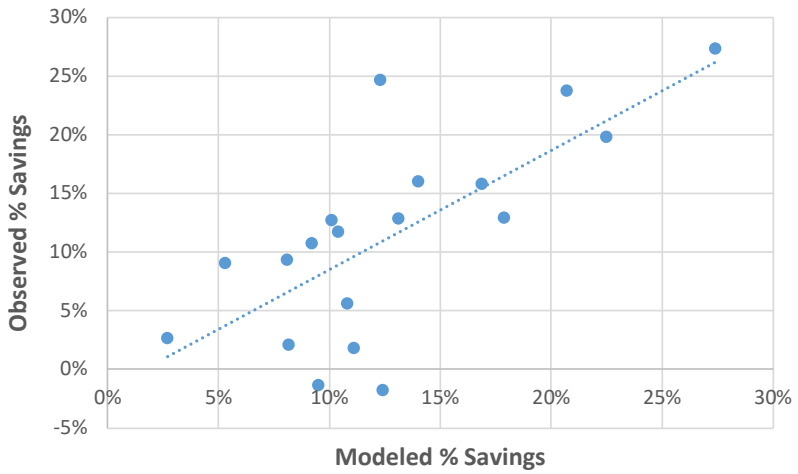

Figure 27: Comparison of modeled and observed savings percentages for the 19 OAR curve changes

The absolute values of the predicted and actual savings were 12.8% and 11.3%, respectively, with an average absolute difference of 4.3%. For the 19 changes, the model predicted actual savings for 13 within ±5% and 16 within ±10%. This indicates that the new approach effectively models the energy impact of overheating from boiler systems due to uncontrolled heat flows and the impact of changing OAR curve parameters on energy consumption.

Objective 4: Achieve <3 year payback period for boiler optimization.

Simple payback period (SPP) equals the cost of providing boiler optimization divided by the cost savings from boiler optimization. We discuss each component of the SPP, followed by an SPP evaluation.

Boiler Remote Monitoring and Optimization Costs

Implementation incurs sensor and telecoms costs and labor costs for sensor deployment, ECM opportunity assessment, and field implementation of ECMs. The cost to a client for a basic installation, minus any energy-efficiency program incentives, was approximately $7,900 at the time of analysis. This cost includes all materials; labor for installation, configuration, and a single optimization analysis[24]; written recommendations, settings optimization and identification of items needing repair[25]. The cost also includes delivery of key alerts, such as 'Not enough heat being delivered to the building' for the duration of the three-year contract.

[24] After optimization of system settings, NEI enters the new settings into the database. A script flag and send internal alerts if the systems operate outside of those new settings. NEI staff makes inquires to determine the circumstances around the changes and determines the appropriate action going forward.

[25] Repairs are indicated in almost all deployments. An example of a frequent repair made is replacement and/or relocation and/or shielding of the system OA sensor. The contract fee excludes repairs, i.e., the client pays for repairs as needed (less any relevant EE program incentives).

Table 5: Representative Cost Breakdowns for a Three-year Deployment

Process Stage	Category	Current Costs[26]	Target Cost
Deployment	Material Cost, $	$1,400	$1,400
	Labor Cost, $ (@ $135/hour)	$2,000	$2,000
	Deployment Total	$3,400	$3,400
Monitoring	Data/Cell Fees for Three Year	$700	$700
Analysis thru ECM	Labor Cost, $ (@ $135/hour)	$1,350[27]	**$540**
ECM Implementation	Labor Cost, $ (@ $135/hour)	$1,350	$1,350
Overhead / Admin.	16%	$1,100	$970
	TOTAL COST	$7,900	$6,960

Simple Payback Period: We evaluated the space heating and DHW gas consumption of nine multi-family properties with 12 to 44 units. On average, they consumed just under $11,000 per year for space heating and $7,000[28] per year for DHW heating, respectively. Fifteen percent savings for both space and DHW heating yields about a 2.6-year SPP based on energy alone.

Based on these findings at the time, coupled with the demonstrated ability for the tool to accurately identify ECMs that could collectively achieve 15% in savings, this objective's criteria had been met. However, much has changed since then.

It is very difficult to tell what the payback period would be if we were to attempt the same analysis today. This is primarily due to the uncertainty of the implementation cost. New Ecology, Inc. for example, is no longer installing its Remote Monitoring systems based on the DAQ spec that formed the basis of obtaining the data used in the project. Beginning during the COVID-19 pandemic, supply chain issues led to several issues and challenges for the hardware stack used in the DAQ systems. Rising hardware and labor costs have certainly increased the base cost for installing and obtaining the data required to use the FDD tool. Given the testing we have already completed to demonstrate cost-effectiveness, we are confident that using the FDD tool to optimize a boiler system will remain cost-effective, should a data acquisition system already be in place on site. The cost of natural gas had also risen during the same time frame, therefore the increased savings in terms of costs could also mitigate some of the increase in base price[29]. The

[26] These costs were captured as part of the study in October 2021.
[27] As noted in the initial proposal to DOE, this represents a decrease from 16-20 hours/site to 10.
[28] Based on $1.20/therm.
[29] https://www.eia.gov/dnav/ng/ng_pri_sum_a_EPG0_PRS_DMcf_a.htm

initial cost of data acquisition could be quite high, though a thorough analysis of existing commercially available DAQ systems was not within the scope of this project.

Another factor is that the market has transformed rapidly in the years since this project was first conceived. Decarbonization and Electrification measures are now at the forefront of discussions with many multi-family building owners. Therefore, the previously conceived longevity of gas-fired boilers may no longer be a valid assumption. With potential replacement of gas boilers on the horizon, the increased cost of data acquisition may not yield a payback period short enough to warrant implementation prior to electrification.

One thing that is important to note and is relevant to evaluating a payback period, is the anticipated persistence of any ECM implementation. As discussed in the introduction, the heating and mechanical systems found in multi-family buildings tend to have a history of reactive maintenance. When making adjustments to an OAR heating curve that could alter the supply temperature of the radiators in conditioned spaces, there is a risk that reduced heat output would lead to tenant complaints thus resulting in an override of the optimized settings.

Given that the primary data inputs for the FDD tool are sensors on the central heating plant equipment only, the heating curve analysis cannot account for actual space temperature conditions. To address that, we collected data from two buildings, using in-unit temperature data loggers to assess the effects of implementing the ECMs identified with the FDD tool. The findings from that study can be found in Appendix B.

Path Forward and Concluding Thoughts

Throughout the development of the beta version of the FDD tool during Phase 2, we added many new features to the software.

While the vast majority of the features for analyzing data collected on Heating and Domestic Hot Water systems with condensing gas boilers have been included, the recommendations for future improvements on this work can largely be broken down into three different categories:

1. How the tool is accessed and used
2. Where the data is sourced for running the tool
3. What systems the tool can be used with

Improving the user interface

Currently, in its beta form, the FDD tool must be used by an engineer who is comfortable with setting up a software development environment and interacting to an extent with python code. In a commercially available tool, a graphical user interface should be developed that removes all visible code from the end-user. Additionally, the outputs of the tool, rather than being displayed on the same screen as the interface for running the tool, should be made available as a downloadable, formatted report – ideally in PDF and XLSX formats.

The abovementioned improvements are based around the assumption that the primary use of the tool continues to be an occasional analysis of historical data collected for the purpose of compiling a scope of work for changes that should be made to improve the performance of a boiler system. This approach was initially developed as a result of the labor-intensive process to extract the necessary data from the DAQ system, clean the data, and analyze it. An ideal use for this tool, which can automate much of the process, may be to build it into a data acquisition system or monitoring tool. In this scenario, a software system could automate the process of loading new data into the tool, running with pre-set parameters on a scheduled basis, and a model could be trained to identify significant changes in the outputs. These changes could trigger an automated notification to a building owner or an engineer for review. This could allow earlier and targeted fault detection and/or incremental recommendations to a boiler's heating curve.

Opening up the data import system

There are currently two primary data input streams for the FDD tool. The first is a direct connection the time-series SQL database that houses data collected by New Ecology's ReMO system. Due to uncertainty in the long-term viability of the ReMO service, an alternative method was added, allowing the upload of formatted CSV files that could import data from any DAQ system with similar specifications. However, this requires a potential laborious effort on the part of the engineer to export and transform data into the appropriate CSV format.

Given that the system is already designed around multiple data import options, it can be easily modified to include additional data formats. For example, an importer designed to extract trend log data from Building Management Systems could be built that may allow engineers to leverage existing infrastructure to collect data rather than installing separate monitoring hardware. There are also other commercially available monitoring tools with sensor packages comparable to the system this FDD tool was designed to work with. Working with additional vendors could expand the reach of the tool. New Ecology is actively seeking partnerships to develop a commercial version of this tool that could be used in conjunction with other vendors' hardware DAQ systems.

Looking beyond boilers

As referenced in the earlier discussion of Objective 4 and the payback period, we face the question: what is the role that a boiler optimization tool has in a world of rapid electrification and decarbonization?

When we first embarked on this project, high efficiency condensing gas boilers were the most cost effective and carbon efficient way to serve the heating and domestic hot water needs of multi-family buildings. In the past five years, however, the landscape has shifted dramatically, and many more building owners are planning for electrification of their heating and domestic hot water systems, or already have transitioned to some form of a heat pump for space heating or hot water. It is inevitable therefore, that this tool will need to be updated to detect faults in other types of equipment while modeling energy consumption and savings potential from replacing boilers with heat pumps or using a heat pump in a dual-fuel system. This will, of course, require updates to the DAQ system. That being said, the use of the tool in its current version should prove valuable in properly sizing a new heat pump system to replace a heating or domestic host water boiler, and identifying ECMs that can help decarbonize a building over time on the path to electrification.

The experience of New Ecology's foray into producing, installing, and maintaining DAQ systems for the primary goal of boiler optimization has led to many lessons learned. One of the challenges New Ecology faced was that the primary selling point of advanced DAQ systems was related to facility maintenance and not necessarily to potential energy savings. This coupled with the fact that costs for implementing a real-time DAQ system have increased suggest that the future of this tool may rely on data collected from DAQ systems already installed to serve another purpose (i.e., on-board connected boilers, Building Management Systems, Connected Thermostat systems, etc.).

There are several reasons a building owner or operator would choose to install such a system, not necessarily due to ECM implementation. For example, from New Ecology's field work providing technical assistance to multi-family building owners and operators we have observed the following:

- Settings overrides happen all the time, on buildings that are ‘well-managed’ and those that are not. Overrides are observed both with active managers and absentee managers.
- Since the beginning of this project, there has been a significant move to fewer maintenance personnel and more buildings managed per person. These personnel have less time to spend hands on with each building ‘listening’ and getting to know the issues.
- The cost of mechanical equipment maintenance has gone up. Higher tech equipment requires more maintenance and a more specialized skillset. This is happening at the same time that maintenance budgets are being squeezed tighter. Having the detailed data gives the equipment a voice about the issues it is running into, allowing for smarter preventative maintenance and reduced no-heat or no-DHW calls while creating the opportunity for greater and more sophisticated remote management of boiler systems.

This suggests the most likely path forward for the FDD tool we have developed is to develop partnerships with commercially deployed DAQ systems that meet the needs of multi-family building owners and operators. Through these partnerships, the FDD tool could be modified to run in the background, or an export stream of data could be made available to a technical assistance provider to run the FDD tool and provide ECM and savings reports.

References

ASHRAE. 2020. *2020 Handbook: Systems and Equipment*, "Chapter 32: Boilers." ASHRAE Press, Atlanta, GA.

ASHRAE. 2021. *2021 ASHRAE Handbook: Fundamentals*, "Chapter 16, Ventilation and Infiltration." ASHRAE Press, Atlanta, GA.

Davey, M.J. and E.F. Connelly. 2018. "BEMS on a Budget: Energy Savings with Low-Cost Monitoring Systems in Affordable Housing." *Proc. ACEEE Summer Study on Energy Efficiency in Buildings*. Aug.

Hewett, M.H. and G. Peterson. 1984. "Measured Energy Savings from Outdoor Resets in Modern, Hydronically Heated Apartment Buildings." *Proc. ACEEE Summer Study on Energy Efficiency in Buildings*. Aug.

Landry, R., A. Haynor, D. Batkiewicz, A. McFarlane, T. Howlet, C. Meschke, and D. Bohac. 2016. "Expanded Scope Commercial Boiler Tune Ups." Final Report by the Center for Energy and Environment to the Minnesota Department of Commerce, Division of Energy Resources. August.

Landry, R., A. Haynor, D. Batkiewic, A. McFarlane, T. Howlet, C. Meschke, and D. Bohac. 2021. "Expanded Scope Commercial Building Tune Ups." Final Report to the Minnesota Department of Commerce, Division of Energy Resources by the Center for Energy and Environment. 31 August.

Lochinvar. 2019. "Lochinvar Crest Condensing Boiler – Efficiency Curve." Last accessed on 926/2023 from: https://lochinvar.com/lit/332206Crest%20Efficiency%20Curve-with%20data_4%20(1).pdf .

Lochinvar. 2020. "CON>X<US: Remote Connect Installation & Operation Instructions." CNX-I-O_100160920_2000001478_Rev E. August. Downloaded on 9/22/2023 from: https://www.lochinvar.com/products/accessories/conxus-remote-connect/ .

New Ecology. 2018. "Continuous Monitoring: A Low-Cost Path to Improved Performance." Final Report by New Ecology, Inc. to the Massachusetts Clean Energy Center (MassCEC). April.

Roth, K.R. and M. Kromer. 2024. "Using Connected Boiler Data to Accurately Quantify Overheating and Energy Savings from Outdoor Air Reset (OAR) Curve Changes in Multi-Family Buildings." *Proc. ACEEE Summer Study on Energy Efficiency in Buildings*. Aug.

Appendix A. FDD Tool Data Use Requirements

This appendix elucidates tradeoffs between sensor instrumentation cost and FDD tool efficacy, with a goal of identifying cost-optimized sensor packages.

The two primary drivers for sensor instrumentation cost that we investigated are:

- Recommended sensor packages that balance FDD feature set vs cost
- Sensor sample rate that balances FDD tool performance vs cost.

In this document, we develop recommendations for two tiers of sensor package: a "minimum recommended package" that offers a lower-cost entry-level offering, and an "optimal recommended package" that offers a higher-cost, full-featured product offering.

Recommended Sensor Packages

An FDD toolset "feasibility matrix" is shown in Table 1-3: it summarizes the scope of feasible FDD analysis, based on the data available for a given plant type (DHW/Heating/Combination). As indicated, the scope and approach of the FDD analysis varies depending on plant type and data availability. There are certain degenerate cases included in the table (e.g., no OAT or HTWS data available) for which there is insufficient data to perform meaningful diagnostics. In addition, for several additional cases (C3, C4, D3), FDD performance is degraded so as not to justify investment.

From the remaining options - H1/H2, C1/C2, and D1/D2 - we have proposed a "minimum recommended sensor package" and an "optimal sensor package" for each plant type, as show in Table 1-1. The resulting feasibility of downstream FDD toolsets is shown in Table 1-2, where "Y" indicates that the specified module is feasible; "Y*" indicates that it is feasible but performance is affected by the sensor package selection; and "N" indicates the test is infeasible. The "optimal DHW" package, which includes a DHW Flow sensor to support estimation of piping energy loss and therefore energy savings estimates from DHW plant ECMs, has not been tested. It is included here as a potential avenue for future investigation.

Discussion of the motivating factors and impacts of sensor selection is included below.

Table 1-1 Downstream FDD analysis feasibility as a function of plant type and data availability

Case	Plant Type	OAT (1)	HTWS/SST, HWTR (2)	HWS, HWR (3)	HW, DHWS, DHWR (4)	DHW Flow Rate	Firing Rate	State Estimation	OAR Analysis	WWSD / S-W Switch Analysis	Heating Energy Savings (5)	Boiler Cycling	Suboptimal TOUT (6)	DHW Setpoint	DHW Energy Savings (7)
-	Comb/Htg	N	X	X	X	X	X	N/A - Insufficient data for analysis					N	?	?
-	Comb/Htg	X	N	X	X	X	X	N/A - Insufficient data for analysis					?	?	?
C1	Combined	Y	Y	Y	See DHW Plant Entry		Y	**Heating Calls:** Non-zero firing rate + DHW OFF **DHW Calls:** Rising HWS + non-zero firing rate	Y	Y	Y	Y	Y	See DHW Plant Entry	
C2	Combined	Y	Y	Y	See DHW Plant Entry		N	**Heating Calls:** Rising HTWS curve with DHW off OR assumes a heating call every 30 minutes during heating season **DHW Calls:** Rising HTWS +Rising HWS	Y	Y	N	N	Y	See DHW Plant Entry	
C3	Combined	Y	Y	N	See DHW Plant Entry		Y	**Heating Calls:** Non-zero firing rate **DHW Calls:** Not implemented	Y	Y	N	Y	Y	See DHW Plant Entry	
C4	Combined	Y	Y	N	See DHW Plant Entry		N	**Heating Calls:** Non-zero firing rate **DHW Calls:** Not implemented	Y	Y	N	N	Y	See DHW Plant Entry	
H1	Heating	Y	Y	N/A	N/A	N/A	Y	**Heating Calls:** Same as C2 Heating Call **DHW Calls:** N/A	Y	Y	Y	Y	Y	N	N/A
H2	Heating	Y	Y	N/A	N/A	N/A	N	**Heating Calls:** Rising HTWS or once per hr with OAT<60 deg and HTWS below threshold **DHW Dalls:** N/A	Y	Y	N	N	Y	N	N/A
D1	DHW	X	X	X	Y	Y	X	**Heating Calls:** N/A **DHW Calls:** Non-zero firing rate	N/A				N/A	Y	Y
D2	DHW	X	X	X	Y	N	X	**Heating Calls:** N/A **DHW Calls:** Rising	N/A				N/A	Y	N
D3	DHW	X	X	X	N	N	X	N/A - Insufficient data for analysis					N/A	N	N

Notes:

1 - Can be t_out or t_weather_station. Weather station is ideally used for building load-vs-OAT calculations in En. Savings, t_out ideally used for other calcs. Both req'd for Sub-optimal TOUT.

2 - Can be t_htws or t_system_supply, ideally system supply. Including both provides supply- and demand-side feedback for OAR Analysis.

3 - HWR only required for determining DHW priority cfg and estimating energy savings.

4 - Will execute with only one of HW and DHWS; only plants with mixing valve expected to have HW.

5 - Requires HTWR in addition to HTWS as currently implemented. However, HTWR is used only for estimating boiler efficiency as a function of outdoor temperature. This has a minor impact on savings estimates, so we can implement a default value in the event that HTWR is not available.

6 - Requires t_out AND t_weather_station

7 - Not tested, potential future feature set

DELETE THIS PAGE UPON PRINTING
(FORMATTING ISSUE)

U.S. DEPARTMENT OF ENERGY

Office of ENERGY EFFICIENCY & RENEWABLE ENERGY

For more information, visit:
energy.gov/eere/xxxx

DOE/GO-000000-0000 ▪ Month Year

Table 1-6: Recommended Sensor Packages, by plant type

Sensor Package	TOUT	WS	SST	HTWS	HTWR	Firing Rate	HWS	HWR	DHWS	DHWR	HW	DHW Flow
Heating - Min	X	X	X									
Heating - Optimal	X	X	X	X	X	X						
Comb - Min	X	X	X				X		X	X	X	
Comb - Optimal	X	X	X	X	X	X	X	X	X	X	X	
DHW - Min	X	X							X	X	X	
DHW - Optimal	X	X							X	X	X	X?

Table 1-7: FDD Feasibility for sensor package selections. "Y*" indicates that a given capability is feasible, but performance is affected by the sensor package selection.

Sensor Pkg	State Est	Subopt. Tout	OAR Analysis	WWSD / S-W Switch	Boiler Cycling	DHW Setpt	Mixing Valve	Heating Energy Savings	DHW Priority	DHW Energy Savings
Htg-Min	Y*	Y	Y	Y*	N	N/A	N/A	N	N/A	N/A
Htg-Opt	Y	Y	Y	Y	Y	N/A	N/A	Y	N/A	N/A
Comb-Min	Y*	Y	Y	Y*	N	Y	Y	N	N	N
Comb-Opt	Y	Y	Y	Y	Y	Y	Y	Y	Y	TBD
DHW-Min	N/A	N/A	N/A	N/A	N/A	Y	Y	N/A	N/A	N
DHW-Opt	N/A	N/A	N/A	N/A	N/A	Y	Y	N/A	N/A	TBD

Local Outdoor Air Temperature / Weather Station Outdoor Air Temperature (OAT): The minimum viable sensor package should include BOTH a local OAT temperature measurement and weather data from the closest publicly available weather station.

- Local OAT represents the control variable for the boiler's outdoor air reset response.
- Supplementing local OAT with weather station data

System Supply Temperature / HTWS + HTWR: A minimum viable sensor package includes one of system supply temperature or HTWS, ideally system supply temperature. An optimal sensor package includes system supply temperature, HTWS, and HTWR.

- System supply temperature measurements show the temperature that the boiler is controlling to, so offers the best indication of the boiler's response to outdoor air temperature.
- Including HTWS in addition to system supply temperature provides an indication of the supply temperature delivered to the building, which can be used to help tune OAR curve settings.
- HTWR (or more specifically, HTWS-HTWR) is used as part of energy savings calculations to estimate boiler thermal efficiency as a function of OAT, HTWS, and firing rate. In general, changes in boiler efficiency represent a small fraction of pre- to post-ECM changes in energy consumption, so HTWR could theoretically be excluded from the optimal sensor package. However, the marginal cost of the additional point is minimal, so its inclusion is recommended.
- In the absence of firing rate data, either SST or HTWS can be used in combination with OAT to implement state estimation for heating plants; or with OAT and HWS to implement state estimation for combination plants.

HWS/HWR/DHW Pump State: A minimum viable package for combination plants includes HWS. An optimal sensor package includes HWS and HWR for combination plants, and optionally could include DHW pump state.

- HWS is required to disambiguate heating calls from DHW calls during combination plant state estimation. Without HWS available, characterizing OAR and WWSD behavior is challenging because warm weather DHW calls pollute meaningful analysis of heating plant behavior.
- DHW pump state can be used in lieu of HWS to identify DHW calls. However, we found HWS temperature rise is an effective stand-in for DHW pump state, and is less costly to instrument.
- The temperature differential between HWS and HWR is used to estimate DHW pump flow rate and, in turn, DHW load. DHW load is used to (a) distinguish DHW energy from heating energy during energy savings calculations; and (b) flag issues with plants that do not implement a DHW priority mode.

Firing Rate: An optimal sensor package includes firing rate (or equivalent boiler load) data from all boilers.

The optimal version of state estimation for combination plants and heating plants uses firing rate data. In the absence of firing rate, HTWS or SST temperature rise (in combination with HWS data for combination plants) can act as a reasonable proxy for identifying heating calls, but with some loss of performance.

In general, the HTWS derivative method is effective at identifying representative time steps that occur during heating or DHW calls, but less effective at estimating plant run time, and not useful for estimating modulation levels. Said another way, points identified by the HTWS derivative

method as being "ON" have a high probability of being ON; but points identified as "OFF" have a relatively high error rate, particularly during heat season.[30]

Excluding firing rate data has the following impact on FDD functionality:

- **State Estimation:** Minor impact for heating and combination plants.
- **OAR Analysis** is minimally affected by substitution of SST/HTWS for firing rate. Estimating the OAR response from observed data only requires selection of a representative sample of points when the heating plant is active across a broad range of OAT conditions.
- **WWSD/S-W Switch analysis** is feasible, but capability is moderately affected. Rather than precisely estimate duty cycle as a function of outdoor temperature, as is feasible with firing rate available, the tool instead estimates "hours per day that the heating system is active". This provides an useful snapshot of how plant activity changes as a function of OAT, but with much less granularity and precision than is feasible with firing rate data.

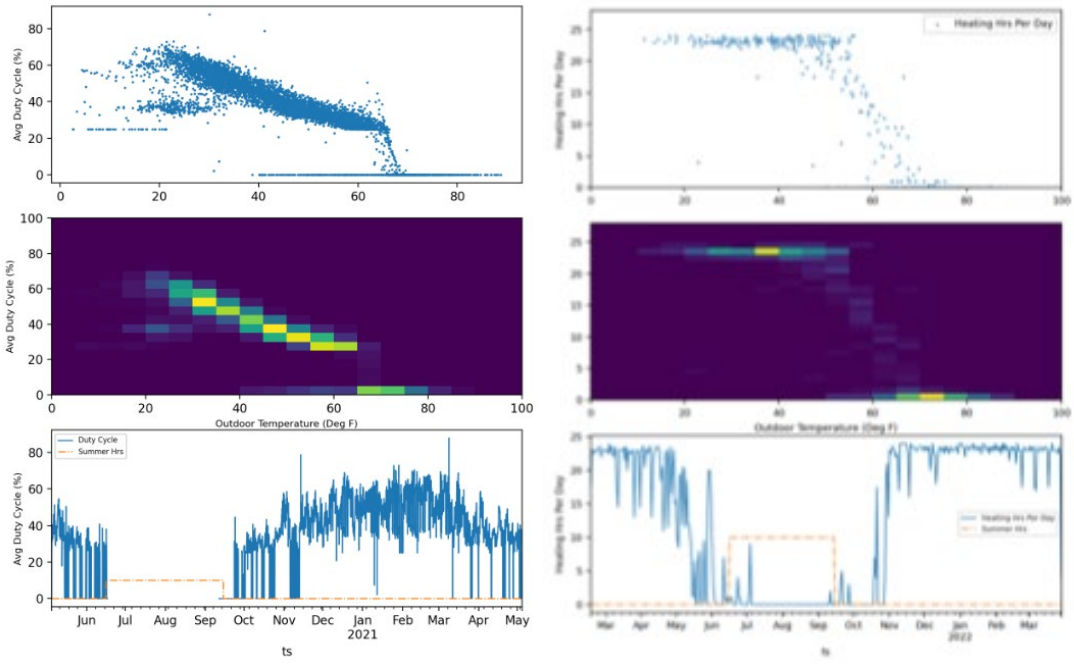

[30] The reason for high error during heating season is that under high duty cycle conditions, HTWS temperature cycling may not be apparent. As such, in the absence of observed cycling, the HTWS derivative method chooses a representative sample of points during cold weather conditions. For OAR analysis, because HTWS does not exhibit cycling, these points will be reflective of the OAR response. However, plant runtimes are not accurately characterized.

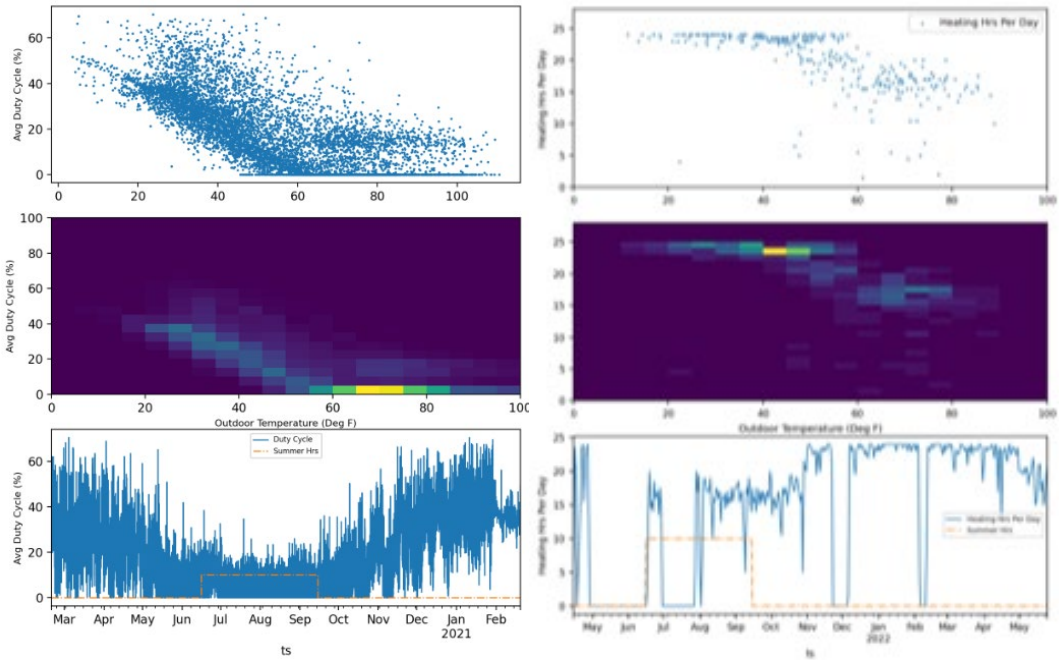

Figure 1-28: Example WWSD plots with and without firing rate data. Left-side: WWSD visualization for plants with firing rate. Right side: WWSD visualization for plants without firing rate. Top Row: Plants with apparently effective WWSD controls; Bottom row: Plants without effective WWSD controls.

- **DHW Setpoint Analysis and Sub-optimal** T_{out} are independent of firing rate data.
- **Boiler Cycling Analysis** is not currently implemented without firing rate data. It is theoretically feasible to identify short cycling during moderate and warm-weather conditions using HTWS derivatives, but this has not been tested.
- **Energy Savings Analysis** is not feasible without firing rate data. Firing rate data is used to estimate building heat load as a function of outdoor air temperature.

DHWR/DHWS/HW: An optimal sensor package includes DHWS, DHWR, and HW for sites with a mixing valve, and DHWR + DHWS for sites without a mixing valve.

- DHWS and HW are used to identify potential mixing valve errors and high/low setpoint issues.
- Including DHWR can help flag potential recirculation pump reversal or mixing valve issues and is minimal marginal cost once DHWS is included.
- Tank setpoint is polled if available, but is not used to flag any fault conditions.

DHW Pump Flow Rate: Estimating DHW energy savings potential by reduced piping loss requires an estimate of DHW demand, which in turn requires flow rate (in combination with DHW supply loop temperature delta, DHWS-DHWR). This functionality is untested, but could be considered as part of a future sensor package.

Sensor Data Rates

Overview

As currently implemented, the FDD tool uses data collected at a 1-minute sample rate for analysis. This sample rate imposes significant costs in terms of data bandwidth, data hosting, and downstream processing.

While there is a real need for 1-minute sample rate data, these needs are constrained to a subset of FDD analyses and can theoretically be consolidated into a single upstream step of the data analysis pipeline. In so doing, we can implement a two-stage data processing pipeline in which data is collected onsite at a 1-minute sample rate, undergoes an initial set of data analysis in near real-time, and then is down-sampled to a 1-hour data rate and posted to a cloud-hosted database for subsequent analysis by the FDD tool.

To be compatible with the proposed two-stage workflow, we need to segregate data analysis into two stages, with the following requirements:

- **Stage 1** – Consumes 1-minute data. Needs to be decoupled from and occur upstream of (i.e., prior to) any stage 2 calculations. In addition, stage 1 data processing will have limited access to historical data: stage 1 should be designed to require no more than 24 hours of high-resolution data. It *can* presumably rely on a limited amount of locally-accessible historical data – ideally this would be constrained to historical averages, etc, but it may be feasible to give access to down-sampled historical time-series data.
- **Stage 2** - Consumes and performs all analysis using 1-hour data.

Table 1-3 audits the data resolution requirements of individual FDD tool modules as currently implemented. These requirements are discussed in detail in the following section.

Table 1-8: Data Resolution requirements for FDD tool modules

FDD Module	Sample Rate Requirements
Data QC	Requires 1-min data
State Estimation	Requires 1-min data with at least 2-hours of historical context. Requires historical metrics to identify HTWS temperature rise threshold and minimum active HTWS threshold if firing rate data is not available.
Suboptimal Tout	Uses 60-min data. Weather station only available with 60-min time step, so faster is not feasible.
OAR Analysis	Uses 60-min data after dropping points where heating_on is False.
WWSD / S-W Switch	By default uses 1-min data, but has a flag (use_hourly) to use 60 min data with minimal impact
Boiler Analysis - Short Cycling	Requires 1-min data to calculate boiler turn-ons per hour; uses 60-min data for all subsequent calculations
Boiler Analysis - Firing Rate vs OAT	Requires 1-min data for visualization of firing rate vs OAT. Could feasibly be replaced with
DHW Setpoint & Mixing Valve	Currently uses 1-min data to characterize min/max DHWS and HW quantiles. Using 1-hour data reduces the impact of outlying points on the analysis, but effect appears relatively minor. Alternatively, metrics could be modified to keep current approach. Need to investigate DHWR>DHWS error for 1-min vs 1-hr case.
Heating Energy Savings	As implemented, uses 1-min data to estimate boiler efficiency as f(OAT, HTWS, HTWR, firing rate), but resamples to 60-min for all calculations downstream of this. Combination plant analysis requires explicitly de-coupling and pre-calculating heating-associated energy and firing rates from DHW-associated energy and firing rate, with methodology varying depending on DHW plant configuration. Efficiency and energy calculations could occur as part of a real-time down-sample.
DHW Priority	DHW pump flow rate requires a list of standalone DHW call energy use using two different estimation methodologies, calculated from high-rate data. Also requires calculation of DHW and heating loads from high-rate data. Subsequent calculations feasible with 1-hr time step.

Appendix B. Analysis of Indoor Temperatures as a Function of OAR Curve Changes at Two Buildings

Introduction

Prior field testing and modeling demonstrated that the greatest energy savings from outdoor air reset (OAR) curve adjustments that decrease HTWS are generated from reducing uncontrolled heat flows from thermal distribution units (TDUs, i.e., radiators and convectors) that overheat rooms. The higher-than-intended T_{in} effectively increases space heating loads and, thus, space heating energy consumption. Our heat transfer modeling shows that uncontrolled heat flow scales with HTWS- T_{out}, which explains why decreases in HTWS can realize significant decreases in space heating energy consumption – but only if a building has a large portion of heat transfer surfaces with uncontrolled heat flow. Earlier work (e.g., Hewlett and Peterson 1984) showed that T_{in} measured in the corridors of multifamily buildings could decrease by several ºF when HTWS was decreased, and we endeavored to make similar measurements to explicitly link changes to HTWS to changes to T_{in}.

Toward that end, during the 2022-23 heating season NEI deployed extended memory Onset HOBO T+rH data loggers in units of four multifamily buildings where they also implemented OAR curve changes (i.e., HTWS[T_{out}]). No other efficiency measures were implemented over the course of the winter. Due to data acquisition configuration problems, viable data sets were only collected for two sites both before and after the OAR curve changes and one site had a very limited number (three) of loggers deployed.

The table below summarizes the OAR parameters for the periods before (A) and after (B) the OAR curve changes at the two buildings; data were collected each minute. At both buildings, HTWS(T_{out}) was 10ºF higher in Period B than in Period A; thus, the model would predict higher T_{in} values during Period B in spaces with uncontrolled heat flows.

Table 9: OAR curve parameters for periods A and B

	Period A	Period A	Period A	Period B	Period B		Period B
Building	HTWS,max / T_{out},min	HTWS,min / T_{out},max	SH1 Setpoint	HTWS,max / T_{out},min	HTWS,min / T_{out},max	SH1 Setpoint	
#1	180/15	125/65	175	190/15	135/65	185	
#2	165/10	115/70	185	175/10	125/70	180	

Findings

Since the average outdoor air temperatures at the two sites were very similar during the two periods, ~37-38°F, we looked at the average T_{in} values in the monitored spaces to evaluate if there were appreciable differences between the two periods. The two tables below summarize the findings for the two buildings.

Table 10: Building #1 average T_{in} measurements for Periods A and B, all in oF (T_{out},averages: A=37.5, B=37.3)

Unit (Floor)	Period A 12/3/22-1/22/23	Period B 1/24/23-3/21/23	dT	Notes
Unit A (2)	68.3	68.7	0.5	
Unit B (3)	N/A	N/A	N/A	Data through 1/8/23
Unit C (3)	75.4	71.9	(3.5)	Data through 3/17/23
Unit D (4)	80.8	80.8	0.0	
Unit E (5)	81.2	80.8	(0.4)	
Unit F (5)	67.7	66.7	(1.0)	
Unit G (6)	72.8	75.1	2.4	
Unit H (7)	65.7	74.2	8.5	
Unit I (7)	68.9	69.6	0.7	
Average	**72.6**	**73.5**	**0.9**	

Table 11: Building # Tin data for Periods A and B, all in °F (Tout averages: A=37.1, B=38.5)

Unit # (Floor)	Period A 12/6/22-1/22/23	Period B 1/24/23-4/3/23	dT_{in}
Unit A (1)	77.1	77.7	0.7
Unit B (1)	71.1	73.2	2.2
Unit C (2)	72.2	73.4	1.2

Average	73.4	74.8	1.3

As would be expected if there were a nontrivial degree of uncontrolled heat flow in the buildings, the T_{in} averaged among the monitored spaces was about 1°F higher in the period with the higher HTWS(T_{out}), Period B.

We can use the T_{in} and T_{out} measurements, along with an estimate for the balance temperature, T_{bal} (e.g., 10°F less than T_{in}), to quantify the approximate energy impact of the change in T_{in}. The space heating load, Q_{in}, is proportional to ($T_{bal} - T_{out}$). Assuming that $T_{bal} = T_{in} - 10°F$, the increases in T_{in} measured for Buildings 1 and 2 would increase the space heating loads in Period B by approximately 3.6% and 5.3% relative those expected given T_{out} in Period B.

Table 4: Comparison of Building 1 and 2 Change in Space Heating Loads

Building	$T_{in,avg}$ – Period A and B	dT_{in}	Expected % Change in Space Heating Loads
Building #1	72.6 -> 73.5	0.9	3.6%
Building #2	73.4 -> 74.8	1.3	5.1%

NEI did not collect connected boiler performance data concurrently with the T/rH that would allow quantification of the extent of overheating and the actual change in Q_{in} .[31] versus T_{out} for each site. However, the room-level data may allow us to determine if the TDUs in a particular unit exhibited evidence of uncontrolled heat flows.

The Figure below shows T_{in} data for Unit A of Building #2. T_{in} appears to have somewhat greater variability during the first period (with lower HTWS), exhibiting periodic spikes. Interestingly, T_{in} approached 95°F late during the evening of February 4th when T_{out} ~13°F, toward the end of a historically cold (T_{out} ,min = -9°F) polar vortex event on February 3rd and 4th of 2023. Unit C also experienced large swings in T_{in}, including during the same event (e.g., from ~70°F in the morning to 84°F around 1PM).

[31] Based on multiplying the boiler firing rate data by estimated boiler efficiency.

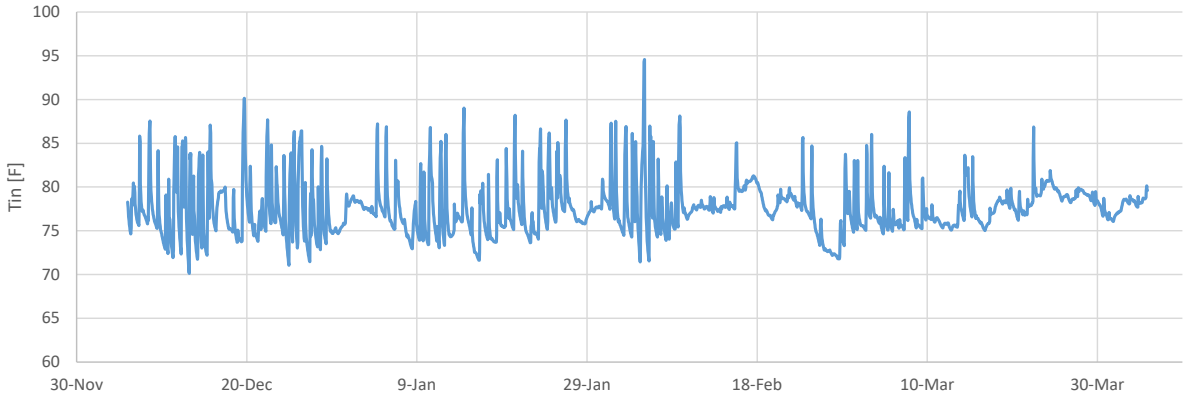

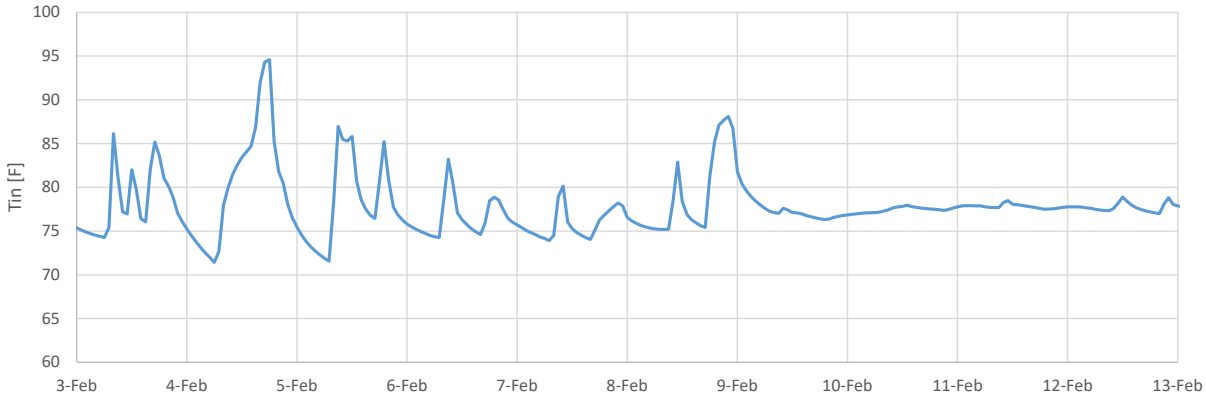

In contrast, the unit with the greatest increase in T_{in} experienced much smaller T_{in} swings, including during the polar vortex event on February 3rd and 4th (see below). There was no clear pattern for how T_{in} varied as a function of T_{out} at Building #2.

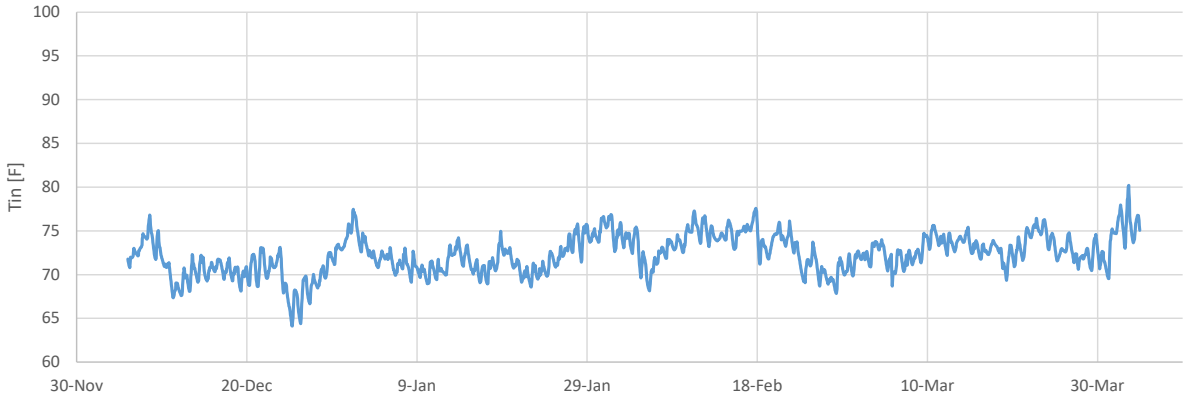

Looking at the unit-level data for Building #1, the data for Unit D show appreciable variability, although the average T_{in} values did not change between periods. Note that the HDUs had plenty of capacity during the early February polar vortex, with average T_{in} on those days exceeding 80°F.

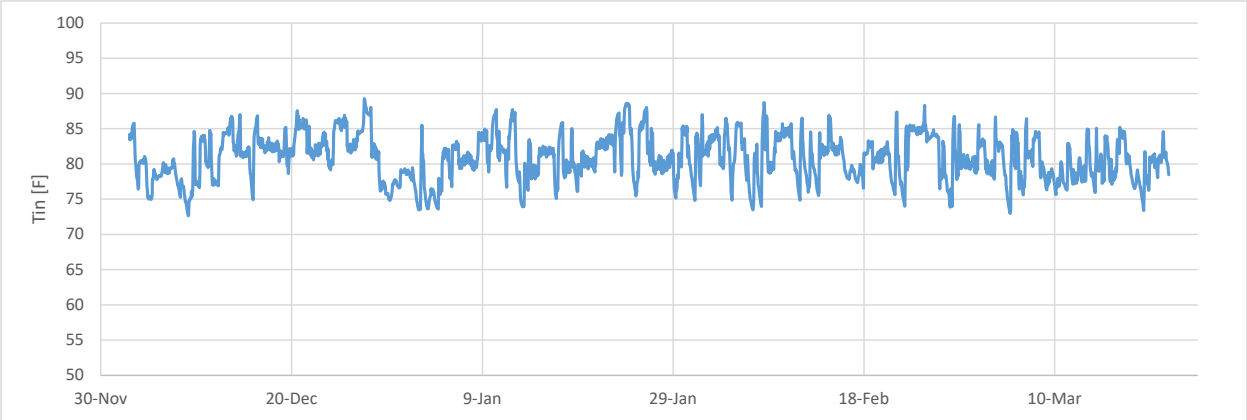

Unit A also had a smaller (~0.5°F) dT_{in} between the periods but a much lower average T_{in}, ~68-69°F.

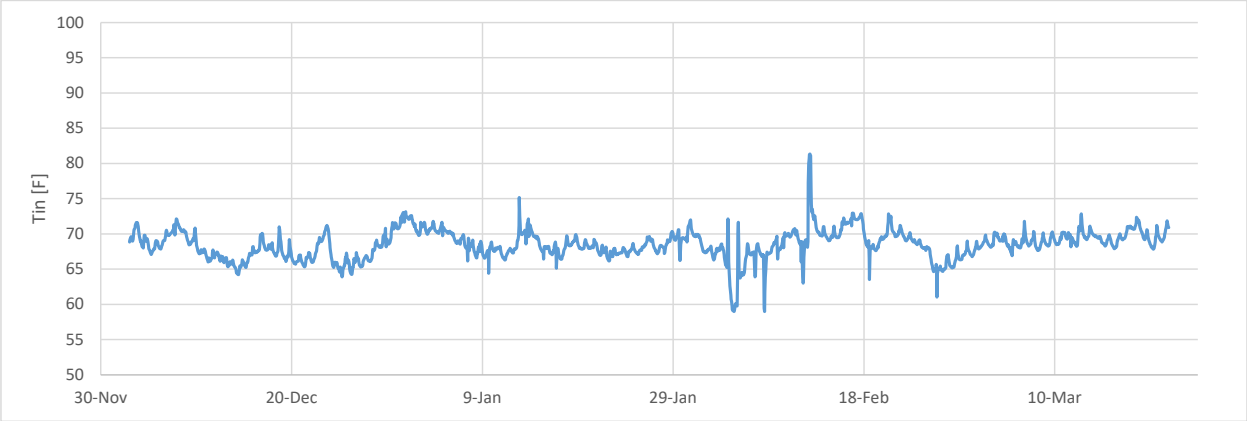

In contrast to Unit D, during the polar vortex T_{in} in Unit A dropped just below 60°F for much of the day, but then recovered. This could be consistent with either an inability of the heating system to keep up under the extreme cold conditions or an increase in the set-point temperature that afternoon.

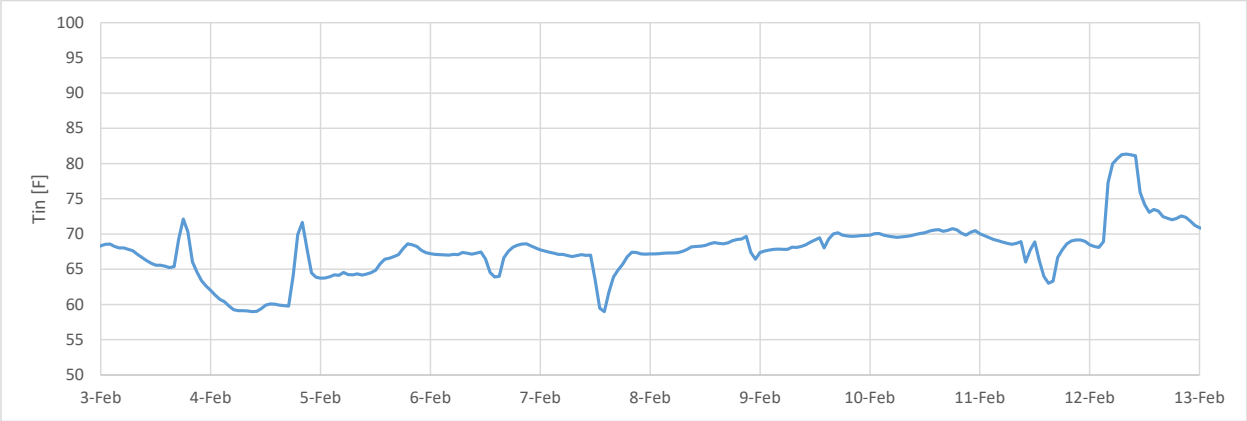

Despite having much higher average T_{in} values (~80ºF), Unit E (below) also had a small (0.4ºF) dT_{in} between periods A and B and low levels of T_{in} variability. During the polar vortex, T_{in} dropped to ~75ºF. Taken together, it appears that this unit had effective T_{in} control but could not quite keep up with T_{in} expectations during the extreme cold of February 4th.

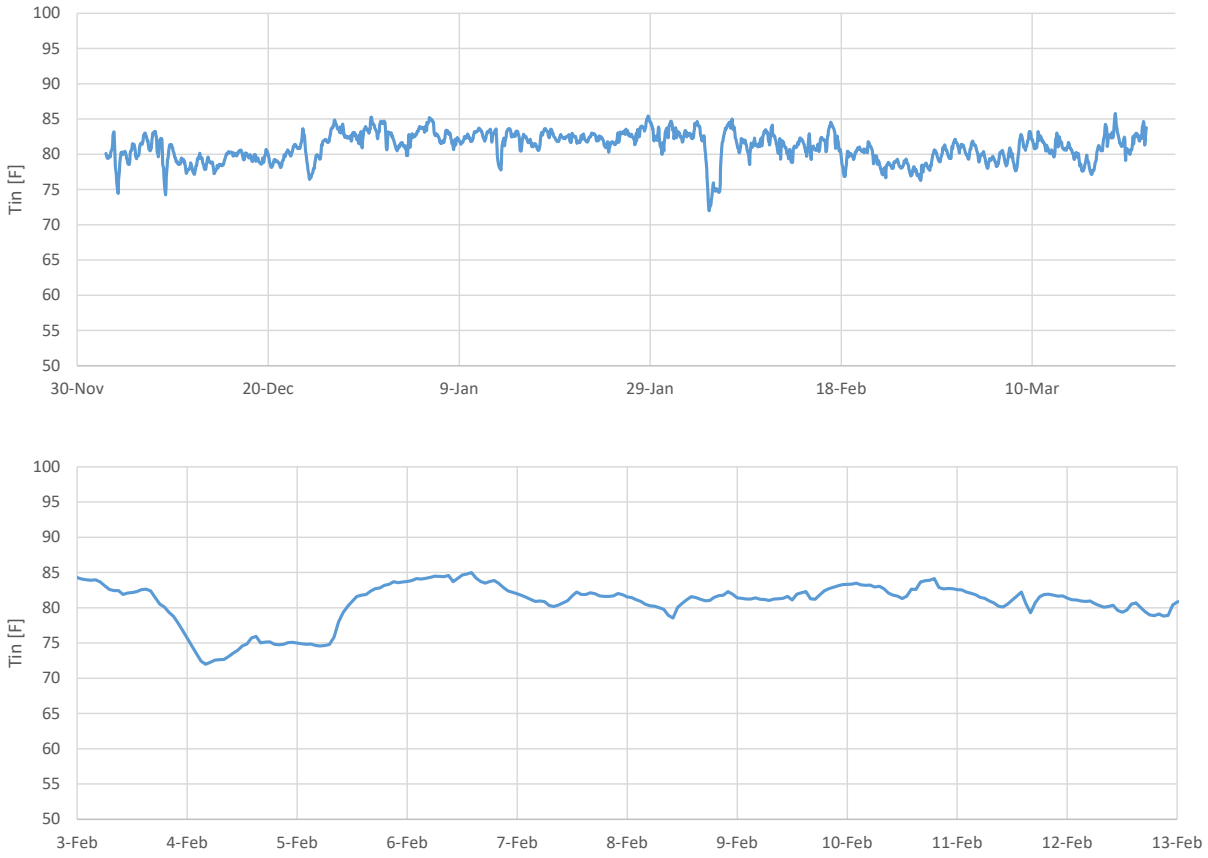

For another unit on the same floor, Unit F (below), the T_{in} values showed appreciably more variability, albeit around a much lower (~67ºF) average temperature. During the polar vortex, T_{in} fell below 60ºF during the coldest part of the day (before noon) but recovered to its ~typical range sooner than in other units.

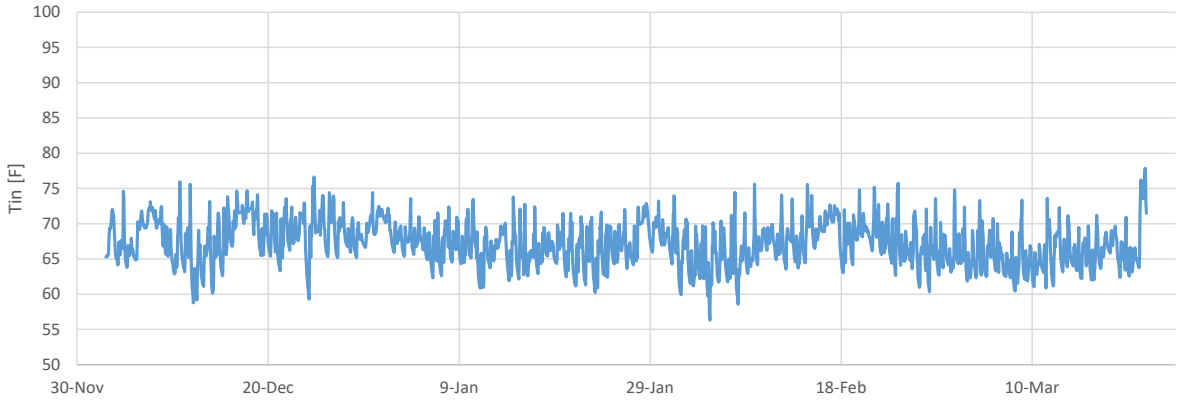

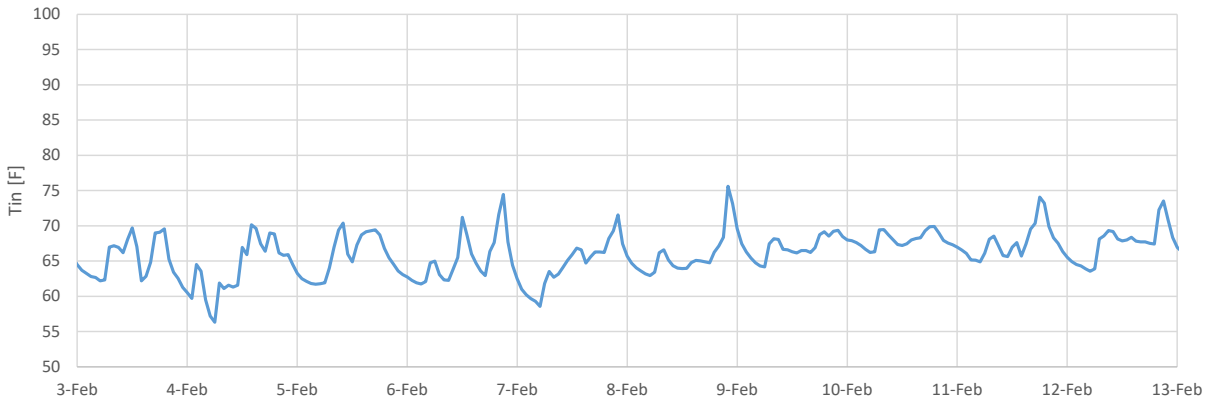

We also examined Unit H, which exhibited the greatest (~8.5°F) increase in the average T_{in} when HTWS was increased during period B, as the very large dT_{in} suggests it had a high degree of uncontrolled heat flow.

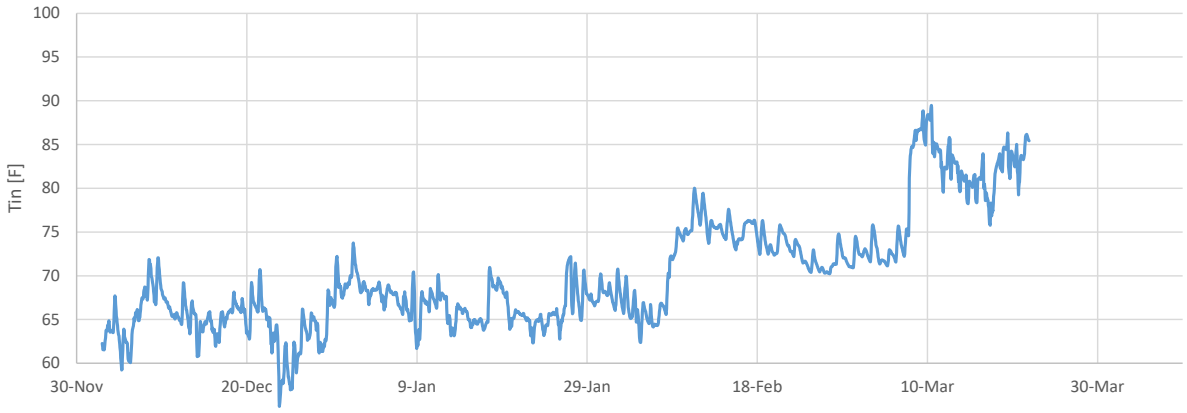

Surprisingly, the increase in T_{in} did not coincide with the OAR curve parameter changes (implemented on 1/23/23) but occurred later, i.e., T_{in} average rose from ~65°F on 2/6/23 to >77°F on 2/10/23. Later, the daily average T_{in} rose from ~72°F on 3/5/23 to ~86°F on 3/8/23. These significant jumps in T_{in} suggest two potential scenarios: 1) changes to in-unit TDU control; and/or 2) uncontrolled heat flow and deviations from the planned OAR curve change. For example, the ~flat average T_{in} after the 1/23/23 OAR curve change indicates effective HDU regulation or that the OAR curve was not fully implemented, while the large T_{in} increases noted in early February and March would be consistent with uncontrolled heat flow combined with unrecorded changes in OAR curve parameters and/or set-point changes reflecting a change in comfort preferences or tenants.

Unit H was located on the top (seventh) floor of the building, so perhaps roof-driven heat transfer affected T_{in}. However, another unit on the same floor (Unit I) showed a much smaller change in T_{in} (~0.7°F) and variability in T_{in}:

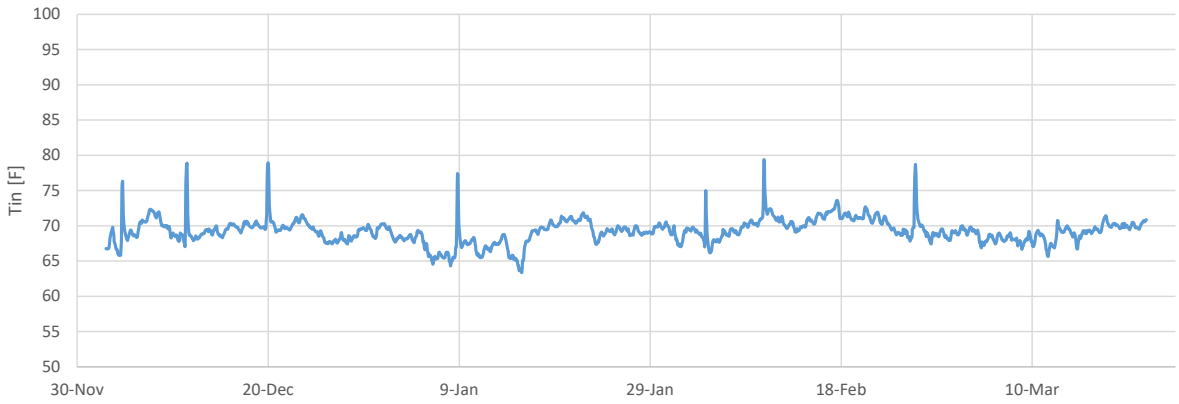

Finally, we examined the T_{in} behavior in Unit C, the one unit in Building #1 that experienced a significant T_{in} (3.5ºF) *decrease* in period B. Given that increases in HTWS(T_{out}) should increase uncontrolled heat flows while controlled heat flows should not change, we found this change surprising. The T_{in} data suggest smaller (1-2ºF) variations in T_{in} around a ~75ºF set point until ~mid January, i.e., well before the OAR curve change. After then, much larger (up to ~10ºF) swings in T_{in} occur and the average T_{in} decreases. While the decrease in T_{in} (T_{out}) would be consistent with better control of heat flows, the large increase in T_{in} variability is not. Potential explanations include significant changes in T_{in} preferences occurred in mid-January (e.g., change in occupancy), a change in HDU effectiveness (e.g., from inhabitant's belongings), and/or a change in thermostat effectiveness (e.g., thermostat exposed to solar heat gains).

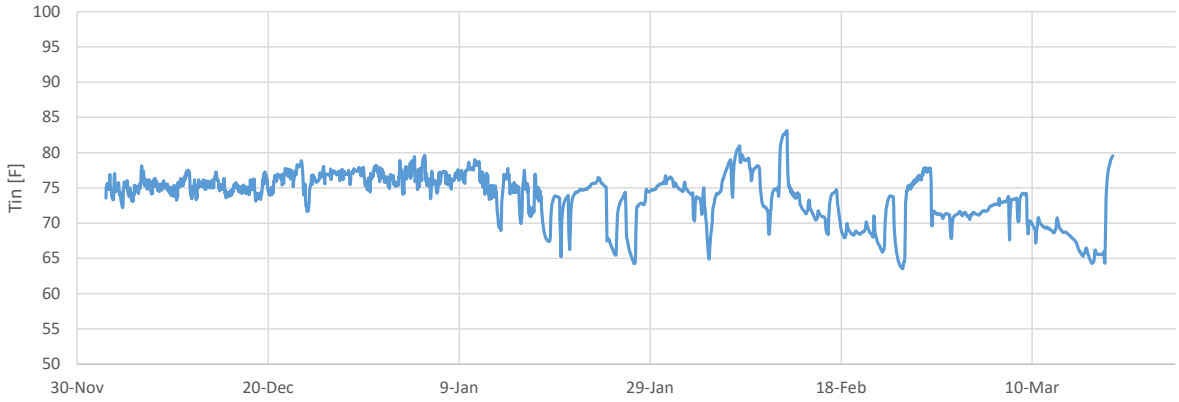

Taken together, these measurements indicate that a random sample of T_{in} measurements from a small portion of units in a multi-family building cannot provide much insight into TDU regulation and boiler system performance. That is, there are several reasons why changes in T_{in} could occur that cannot be readily understood without additional context. As demonstrated in the energy savings analysis, our methodology to analyze connected boiler data provides much more insight into boiler system performance and the degree of uncontrolled heat flow in a building. Nonetheless, unit-level T_{in} data do provide crucial insights into actual comfort conditions, which can certainly help optimize OAR curve parameters while maintaining comfort.

If it is not possible to monitor T_{in} in most units, we recommend sampling T_{in} data from a larger portion of units and/or measuring T_{in} in common spaces, e.g., central corridors, that would tend to average T_{in} for a given floor.

Appendix C: A Physics-based Model for Hydronic Heat Transfer[32]

The fundamental problem with the existing approaches to quantifying the expected energy savings from changes to the OAR curve is that they do not take into account the actual control of boiler distribution systems in a specific building, i.e., the extent of uncontrolled heat flow-driven overheating that occurs. To address this, we developed a basic model for heat transfer from the hydronic distribution loop to indoor spaces and how heat distribution unit (HDU) control – or the lack thereof – impacts effective space heating loads and boiler energy consumption. Figure 4 shows the basic model for heat transfer to and from a hydronically heated room.

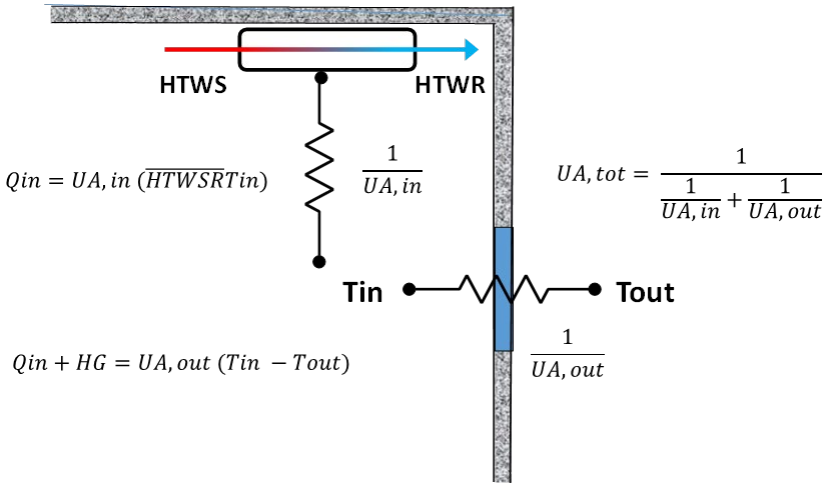

Figure 4: Conceptual model of room heat transfer with boiler system and outdoors.

Heat transfer from the heating loop to the space, Qin, equals:

$$Qin \simeq UA_{in}(\overline{HTWSR} - Tin)VRT \quad (1)$$

where the variables are:

- HTWS: Heating loop supply water temperature, i.e., temperature entering the radiator/convector (from now on referred to as a heat distributing unit, or HDU).
- HTWR: Heating loop return water temperature, i.e., temperature leaving the HDU.
- $\overline{HTWSR}$: The average of HTWS and HTWR, i.e., 0.5*(HTWS + HTWR)

[32] This appendix is an excerpt from Roth and Kromer 2024.

- Tin: Room temperature.
- UA_{in}: the overall heat transfer coefficient for an HDU, which varies as a function of HTWS and Tin.
- VRT is the % of time the thermostatic valve (TV) is open.

A heat balance on the fluid flowing through the HDU shows that the change in flow thermal energy equals the heat transferred to the space; here, *m* equals the water mass flow and cp the water thermal capacitance:

$$mc_p(HTWS - HTWR) = UA_{in}\,(\overline{HTWSR} - Tin) \quad (2)$$

Similarly, the overall heat balance for the room equals:

$$Qin + HG = UA_{out}(Tin - Tout) \quad (3)$$

where HG equals internal plus solar heat gains while UA_{out} is the overall heat transfer coefficient from the building to the outdoors from conduction, radiation, and infiltration.[33] When Qin = 0, i.e., when Tout equals the balance temperature, Tbal, at the indoor design temperature, Tin,design:

$$HG = UA_{out}\,(Tin, design - Tbal) \quad (4)$$

At Tbal, internal and solar heat gains exactly balance heat losses from conduction and convection, i.e., space heating is required below Tbal.[34]

Once values for some variables are known or estimated, we can solve for the other variables. For example, if we can estimate Tin,design, Tbal, and UA,out, and assume VRT = 100% at design conditions, we can solve for UA,in (at design conditions) and *m*:

$$UA_{in} = \frac{UA_{out}\,(Tbal - Tout,design)}{\overline{HTWSR(Tout,design)} - Tin,design} \quad (5)$$

$$mc_p = \frac{UA_{in}\left(\overline{HTWSR(Tout,design)} - Tin,design\right)}{\overline{HTWSR(Tout,design)}} \quad (6)$$

[33] This basic HDD formulation (i.e., PRISM) for space heating loads lumps conduction and infiltration heat losses into a single UA term, assuming both conduction and infiltration vary linearly with Tin – Tout. Actual building infiltration tends to exhibit appreciable nonlinearity, with an average exponent of ~0.65 (ASHRAE 2023).
[34] In practice, Tbal can vary appreciably depending on the actual SHGs experienced by a building, as well as with nonlinear wind-driven infiltration.

The temperature difference for the water flowing through the HDU, dT, at other conditions equals:

$$dT(HTWS, Tin) = HTWS - HTWR \cong dT_{design} \frac{(HTWS[Tout] - Tin)}{(HTWS,design - Tin,design)} \frac{UA_{in,new}}{UA_{in,design}} \quad (7).$$

The last term takes into account that HDU output scales with $(HTWS\text{-}Tin)^n$, so UA_{in} scales with $(HTWS - Tin)^{n-1}$, where n depends on the type of HDU. Based on ASHRAE (2020), n = 1.31 for baseboard units (1.375 for SlantFin products) and 1.2 for cast-iron radiators. Although Tin decreases as HTWS decreases (assuming VRT is constant), the change in Tin is typically small relative to that in HTWS (see subsequent discussion).

To model how boilers can inadvertently overheat spaces, we next discuss system performance with controlled and uncontrolled heat transfer from the boiler distribution system to the room.

Well Controlled Case

Thermostatic valves (TVs) regulate heat flow from the boiler supply loop to rooms that shut off water flow through the HDU when the room achieves[35] its target temperature set-point, Tset. That is, TV *should* turn on and off the valve such that Tin ~equals Tset. In that case, for any HTWS and HTWR, the space heating load, Qload, and the controlled Qin, Qin,contr, both decrease linearly from the heating load at Tout,design, Qin(Tout,design), to Tbal:

$$Qload = Qin, contr = UA, out(Tin - Tout) - HG = UA, out\ (Tbal - Tout)$$

$$= Qin\ (Tout, design) * \frac{(Tbal - Tout)}{(Tbal - Tout, design)} \quad (8)$$

Uncontrolled Case

If the TV does not modulate effectively to control heat flow to the space, e.g., if the TV is stuck open, the dynamics change appreciably as the heat flows continuously from the boiler system into the room, i.e., VRT = 1.0 *under all conditions*. Since Tin is no longer controlled, it increases to an equilibrium temperature, Tin,eq, where the heat flows balance:

$$Qin + HG = UA_{in} mcp\ dT + HG = UA, out\ (Tin, eq - Tout) \quad (9)$$

[35] Or, in the case of thermostats with anticipation action, approaches Tset.

Qin now equals the uncontrolled heat input into the space, *Qin,uncontr*, which is proportional to the difference between $\overline{HTWSR}$ and Tout:

$$Qin, uncontr = Qin = UA, out\ (Tin, eq - Tout) - HG. \quad (10)$$

Viewed another way, in the uncontrolled case heat transfer from the HDU at $\overline{HTWSR}$ to the outdoors at Tout occurs through two heat transfer resistances, $1/UA_{in}$ and $1/UA_{out}$. The total UA, UA,tot, equals:

$$UA, tot = \frac{1}{UA_{in}(Tout)} + \frac{1}{UA_{out}} \quad (11)$$

Consequently, Qin,uncontr is approximately proportional to the difference between HTWS and Tout:

$$Qin, uncontr\ \sim UA_{tot}(HTWS - Tout)\ C_{TV}. \quad (12)$$

Here, the C_{TV} factor takes into account how UA,in varies as a function of the difference between $\overline{HTWSR}$ and Tin,eq (see prior discussion and Appendix A). This expression neglects both internal heat gain and the reality that heat transfer between the HDU and Tin,eq occurs at $\overline{HTWSR}$[36]. As shown later, these simplifications do not appear to have a significant impact on the accuracy of data-driven assessments of the degree of overheating from uncontrolled heat flows for a specific boiler system or the predicted energy savings from decreasing HTWS. If we assume that the HDUs would just meet the design heat load as design conditions, i.e., when Tout = Tout,design and Tin(Tout,design) =Tin,design, VRT(Tin,design) = 100%, then Qin,uncontr is also approximately proportional to Qin,design:

$$Qin, uncontr(Tout) \cong Qin, design\ \frac{HTWS(Tout) - Tout}{HTWS(Tout,design - Tout,design}\ C_{TV} \quad (13)$$

[36] Although hydronic systems are often designed for dT~20°F, field data collected by New Ecology for >100 multifamily buildings found that dT did not approach that value for most boiler systems.

We can also solve the energy balance and dT(HTWS,Tin) equations simultaneously to obtain Tin,eq, where $UA_{in,design}$ and $UA_{in,new}$ are calculated for the HDU at the design and new HTWS values:

$$Tin,eq = \frac{UA_{out}Tout + HG + \frac{mcp\ HTWS\ dT\left(HTWS_{design}, Tin_{design}\right) UA_{in,new}}{\left(HTWS_{design} - Tin_{design}\right) UA_{in,design}}}{\left(UA_{out} + \frac{mcp\ dT\left(HTWS_{design}, Tin_{design}\right) UA_{in,new}}{\left(HTWS_{design} - Tin_{design}\right) UA_{in,design}}\right)} \quad (14)$$

Unsurprisingly, a perpetually open TV can significantly increase indoor temperatures. Figure 5 shows Tin,eq as a function of Tout based on this methodology based on the following assumptions: Tdesign = 0°F; Tset,design = 75°F Tout; VRT(Tout,design)=100% (for the controlled case); HG = 10°F and a HTWS reset curve of (10,180) and (60,120).[37] In that case, our model shows the building experiences significant overheating, with the expected Tin,eq often exceeding 80°F. Heat transfer from the room to the outdoors, which scales with Tin-Tout, increases, so effective space heating loads do as well.

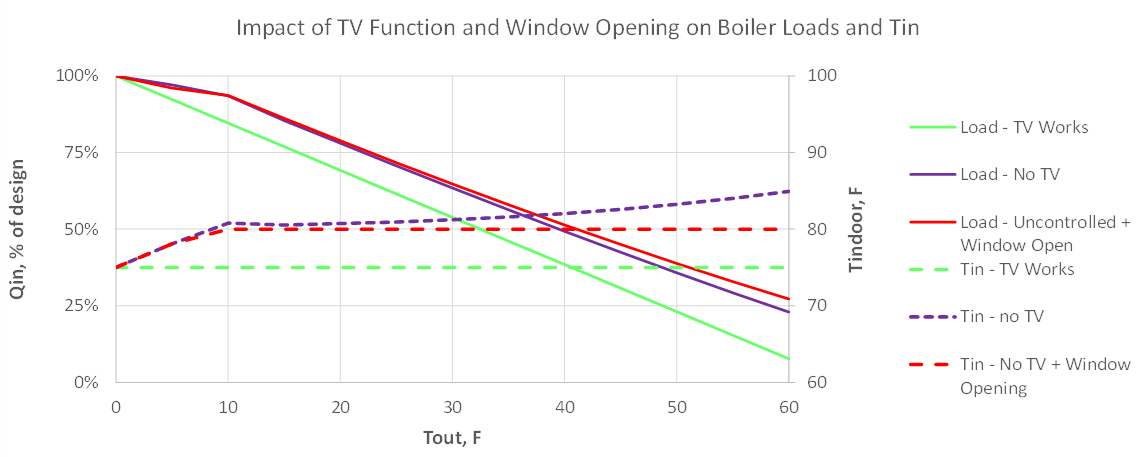

Figure 5: Example of modeled Tin and boiler output (Qin) as a function of Tout for three control scenarios: TV Works, No TV (= failed TV), No TV + Window Open.

Elevated Tin,eq makes it more likely that inhabitants will open windows to moderate Tin, which increases UA_{out} and UA_{tot} for the entire system. We can estimate the increase in UA_{out} by

[37] The first term of the reset curve parameters specifies Tout (10°F) when HTWS reaches its maximum value (180°F) while the second specifies the Tout (60°F) when HTWS reaches its minimum value (120°F).

assuming people would operate windows to achieve a maximum, marginally acceptable indoor temperature, Tin,max, In that case, the window-controlled Tin, Tin,cont, equals:

$$Tin,cont = MIN\ (Tin,equ\ ,\ Tin,max). \quad (15)$$

Since Tin is now fixed and VRT = 100%, we can readily solve for dT and then $UA_{out,new}$ from a room energy balance:

$$dT = dT_{design} \frac{HTWS - Tin,cont}{HTWS_{design} - Tin_{design}} \frac{UA_{in,new}}{UA_{in,design}} \quad (16)$$

$$UA_{out,new} = \frac{mcp\ dT + HG}{(Tin,cont - Tout)} \quad (17)$$

Calculations made for $UA_{out,new}$ indicate that UA_{out} increases ~10-15% when Tout ~25-30°F, and by >40% when Tout is 50°F relative to the windows closed case.

Estimating the Fraction of Controlled and Uncontrolled Heating Energy Consumption

As shown, uncontrolled heat flow can greatly increase Tin, effective building loads, and boiler energy consumption. We now present an approach that uses data from connected boilers to estimate the *degree* of overheating occurring in a building. Connected boilers acquire a range of time-series data about boiler performance, such as boiler firing rates (BFR), outlet and return temperatures, status and error codes, etc. and communicate it to the cloud. Building operators can then access those data remotely (see Lochinvar 2023). *We use the $\overline{HTWSR}$, FiringRate, and Tout data from connected boilers to evaluate the degree of overheating occurring for a specific boiler system.*

As shown earlier, a building with well-regulated heat flows from the boiler system will result in space-heating *loads* that decrease approximately linearly from Tout,design to Tbal. In contrast, space heating loads in buildings with uncontrolled Tin regulation will scale with ($\overline{HTWSR}$ – Tout), with an abrupt drop-off around the warm-weather shut-down (WWSD) temperature (when the system automatically locks out the boiler from firing). **Thus, we can analyze the *shape* of the boiler gas consumption (derived from BFR data) versus Tout curve to identify systems that have appreciable overheating. Specifically, we expect boiler plants with Load (= Qin * η) vs. Tout slopes that scale with ($\overline{HTWSR}$ –Tout) and do not converge to negligible**

average BFR (i.e., negligible space-heating gas consumption) at Tbal (e.g., around ~55-65°F) indicate significant overheating.

Uncontrolled heat flow yields a gas consumption vs. Tout curve similar to that shown in Figure 2 from Hewett and Peterson (1984), who reported Tin values in many buildings they investigated ranging from the mid-70s to mid-80s, indicative of significant overheating relative to typical design temperatures and likely window opening.

In practice, many buildings have a mix of controlled and uncontrolled heat flow from HDUs. Then, the actual Qin to the building, Qin,actual, equals the product of the controlled and uncontrolled cases with the fraction of HDU UA associated with each case, where SC equals the fraction of HDUs with well-controlled heat flow.

$$Qin, actual = SC * Qin, contr(Tout) + (1 - SC) Qin, uncontr(Tout, HTWS) \quad (18)$$

Figure 6 show conceptually to apply these basic models to estimate the actual extent and energy impact of overheating in a building by comparing actual average hourly heating loads at different Tout values to the fully controlled and uncontrolled cases. As in Figure 2, the upper red line represents the Qin(Tout) curve for the uncontrolled case, the lower green curve the controlled case, and the middle blue line a curve for an actual boiler system with some fraction of uncontrolled heat flow, *SC(Tout)*. As noted earlier, this assumes that the controlled (i.e., ideal) and uncontrolled curves converge at Tout,design, i.e., that the HDU TVs are always fully open to attain Tin,design at Tout,design. For the analysis that follows, this is likely a conservative assumption for many buildings that have spare boiler and HDU capacity at design conditions.

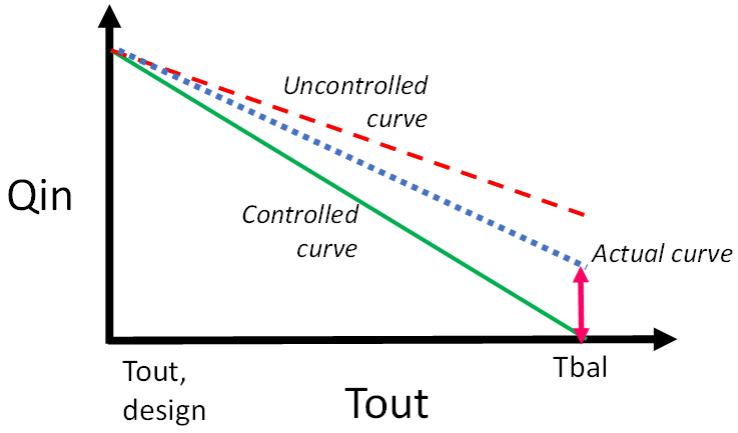

Figure 6: Conceptual diagram of boiler Qin versus Tout curves for ideal HDU control and uncontrolled HDUs, with an example of an actual boiler system with uncontrolled heat flow in ~60% of spaces.

Modeling Energy Impact of Uncontrolled Heating Energy Consumption and OAR Curve Changes

Using BFR and HTWS data from connected boilers and Tout weather data, we can assess SC(Tout) for each 5°F Tout bin by calculating the difference between Qin,actual and Qin,ideal(Tout) divided by the difference between Qin,uncontr(Tout) and Qin,contr(Tout) given the boiler system's HTWS(Tout):

$$SC(Tout) = \frac{Qin,actual(Tout) - Qin,contr(Tout)}{Qin,uncontr(Tout) - Qin,contr\ (Tout)} \quad (19)$$

We can then calculate Qin for any conditions:

$$Qin(Tout) = Qin(Tout, design)\left[\frac{SC * C_{TV} * (HTWS(Tout) - Tout)}{HTWS(Tout,design) - Tout,design} + \frac{(1 - SC)\,(Tbal - Tout)}{Tbal - Tout,design}\right] \quad (20)$$

We can use this expression to model and predict the energy impact of changes to the OAR curve parameters, i.e., HTWS(Tout). *Crucially, changes in HTWS(Tout) only result in savings from reducing overheating in portions of the distribution system with uncontrolled heat flows, as system portions with well-controlled heat flows effectively modulate Qin as loads change.*[38] Consequently, systems with load curves closer to the uncontrolled case can achieve significant overheating/load-related savings, as decreasing HTWS directly decreases Qin for uncontrolled flows. In contrast, systems with load curves closer to the controlled case will realize smaller savings from the same OAR curves, since a smaller portion of the heat distribution is uncontrolled. Figure 7 show an example of this approach applied to two OAR curves, with Tbal = 60°F and SC = 0.59; the actual SC would be calculated using BFR data.

[38] In the extreme case where heat flow is perfectly controlled, the savings from modifying the HTWS curve are driven entirely by nominal changes in boiler efficiency as a function of temperature and firing rate.

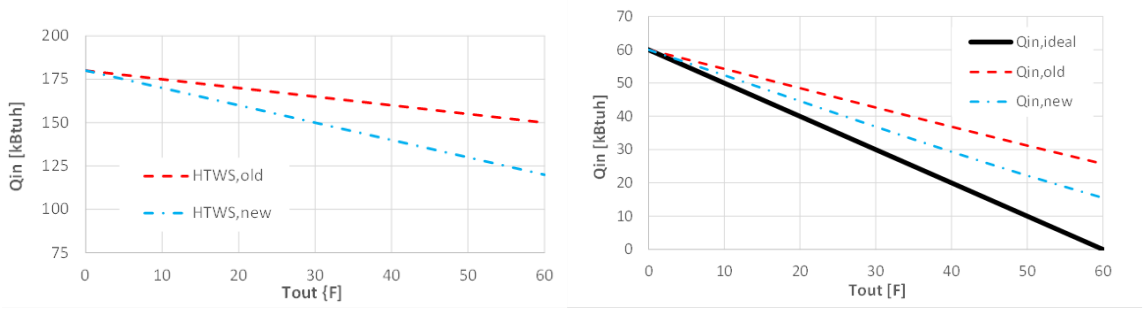

Figure 7: Modeled example of how lowering HTWS (Tout; *left*) decreases Qin,uncontr(Tout), shown relative to ideal (controlled) case (*right*).

Assuming the portion of the system with uncontrolled heat flows does not change when HTWS(Tout) changes, e.g., due to window opening, we can estimate the reduction in space-heating heat into the building from changes in HTWS for each Tout bin, dQin(Tout), and the percentage change in Qin, OAR,save,load (Tout), taking into account changes in C_{tV}:

$$dQin\ (Tout) = \frac{SC * Qin\ (Tout,design) * \left[C_{TV,fail,old}\ (HTWS_{old}\ (Tout) - Tout) - C_{TV,new}\ (HTWS_{new}\ (Tout) - Tout)\ \right]}{(HTWS(Tout,design) - Tout,design)} \quad (21)$$

$$\%OARsave,load(Tout) = \frac{SC * \left[C_{TV,fail,old}\ (HTWS_{old}\ (Tout) - Tout) - C_{TV,new}\ (HTWS_{new}\ (Tout) - Tout)\ \right]}{(HTWS(Tout,design) - Tout,design) * \left[\frac{SC * C_{TV,old}\ (HTWS_{old}\ (Tout) - Tout)}{(HTWS,design - Tout,design)} + (1 - SC)\left(\frac{Tbal - Tout}{Tbal - Tout,design}\right)\right]} . \quad (22)$$

One thing to note is that if the load curve is linear with Tout and the change in HTWS(Tout), i.e., dHTWS(Tout)/Tout, is constant over a temperature range, the *magnitude* of the hourly savings would be the same for those Tout bins (not accounting for changes in UA_{in} and UA_{tot} that will "bend" down the theoretical uncontrolled load curve). The *percentage* savings will, however, increase as Tout increases, since the magnitude of the baseline load decreases while the quantity of energy saved remains constant. In practice, these calculations can become very sensitive as Tout approaches the estimated Tbal. Since the ideal load becomes small under those conditions,

uncontrolled heat flows likely dominate space heating. Consequently, it may be reasonable to assume that SC = 1 when Tout approaches Tbal.[39]

To obtain a representative estimate of annual savings from the OAR curve changes, we apply the SC(Tout) values to TMY data, multiplying dQin(Tout) for each Tout bin by the hours/year in that bin in a typical mean year (TMY). Any incremental savings from increased boiler efficiency would be calculated based on the difference between Qin to obtain a difference in boiler energy, Qgas, i.e., Qin divided by η(Tout), for the baseline and reduced load cases.

[39] If HTWS were decreased below the minimum required to meet the space heating load at a given Tout, with functioning TVs fully open, Tin would fall below Tin,design. The model assumes that HTWS(Tout) is not decreased to an extent that this occurs.

U.S. DEPARTMENT OF
ENERGY

Office of
ENERGY EFFICIENCY &
RENEWABLE ENERGY

For more information, visit:
energy.gov/eere/xxxx

DOE/GO-000000-0000 ▪ Month Year

U.S. DEPARTMENT OF
ENERGY

Office of
ENERGY EFFICIENCY &
RENEWABLE ENERGY

For more information, visit:
energy.gov/eere/xxxx

DOE/GO-000000-0000 ▪ Month Year